Pilot study:On the distribution of elements throughout the Mount Gunson tailings.

Karen Hulme

Co-operative Research Centre for Landscape Environments and Mineral Exploration.

School of Earth and Environmental Sciences.

University of Adelaide, Adelaide, SA, 5005, Australia.

A paper submitted in the partial fulfilment of the requirements of the Honours degree of Bachelor of Environmental Science

2002

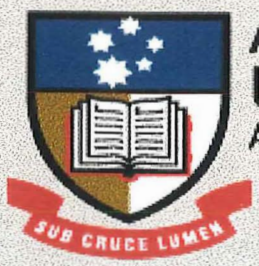

ADELAIDE UNIVERSITY AUSTRALIA

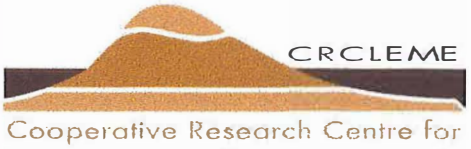

Cooperative Research Centre for Landscape Environments and Mineral Exploration

Abstract

Heavy metals copper, lead, zinc, cobalt and nickel released from the mining and processing of copper-bearing sulphide minerals at the Mount Gunson Cattle Grid district in central South Australia, were studied to determine their geochemical behaviour and distribution in near surface environments in three tailings impoundments. The Cattle Grid mine was in operation during 1972 – 1986, producing approximately 7.4 million tonnes of tailings. This study of the tailings showed that oxidation of sulphide minerals in the upper 2 m of the tailings; coupled with a system dominated by evaporation, lead to the occurrence of water-soluble secondary salts in the oxidation zone, resulting in an average pH of 5. In contrast' element fluctuation within the reduced environment at depths below 2 m is a function of mineral, grainsize partitioning upon deposition, grade of ore being mined and the efficiency of the extraction process resulting in an average pH of 8.

Key words: Mount Gunson • temperature • pH • heavy metals • precipitation • extraction processes

Introduction

During Australia's history sediment-hosted copper deposits have provided approximately two-thirds of Australia's copper production (Lambert et al., 1984). These deposits are characterised by disseminated, commonly zonally distributed sulphides that occur in reduced rocks near oxidation-reduction boundaries (Van Herk et al., 1975). South Australia can be considered as one of the world's major copper belts with deposits in Kapunda, Burra, Wallaroo, Moonta, Olympic Dam and Mount Gunson (Dickson, 1942). Between 1875-1972 several deposits were discovered at Mount Gunson. These deposits are located in the Upper

North of South Australia, approximately 400 km northwest of Adelaide. Mining at Mount Gunson occurred in five main periods: 1898 - 1919, 1941 - 43, 1970 - 71, 1974 - 86 and 1987 – 89. Total production to the end of 1989 contained 149 275 t of copper metal (Tonkin and Creelman, 1990). The largest deposit at Mount Gunson is Cattle Grid, with a major sulfide mineralogy of chalcocite (Cu) > bornite (Cu > Fe) > chalcopyrite (Cu = Fe) > pyrite (Fe) > sphalerite (Zn) > carrollite (Co). Also present are minor sulfide minerals bavoite, arsenopyrite, cobaltite, gersdorffite, glaucodot, marcasite, wittichenite, covellite and idaite (Bampton, 1988).

During the major phases of mining in 1974 - 86, CRS Limited (1974 - 84) and EMAC Partnership (1984 - 86) treated 7.5 Million tonnes of sulphide ore with an average head grade of 1.9 % Cu which resulted in the recovery of 127 000 t copper and 62 000 kg silver (Bampton, 1988).

The recovery of economical minerals was achieved by removal of the overburden, blasting of the exposed ore, crushing, milling and flotation. Using these processes and a 1 % cut off approximate copper recoveries of 94 % were accomplished, which resulted in 7.4 Million tonnes of tailings. It is considered likely that the 6 % loss in metal recovery is reported to be in the tailings. The main heavy metals in the tailings assayed 0.14 % Cu; 0.014 % Co; Fe = 3600 ppm; Zn = 250 ppm; Pb = 200 ppm; Mn = 35 ppm; Ni = 12 ppm; As = 23 ppm and Bi = 7 ppm in a gangue of quartzite, micas and feldspars (Puccini, 1996).

Geochemical studies have shown mine tailings to be of environmental concern, as well as a possible future source for additional revenue through reprocessing. Mine tailings mineralogy is complex and multiphased, and is a function of the type of deposit, grade of ore,

the proportion of sulphides, and buffering capacities of the tailings, as well as local and regional climate (Boulet, Adrienne and Larocque, 1998).

Mineralogical studies of mine tailings are of importance for environmental applications because most ore minerals are very responsive to changes in environmental conditions especially temperature and pH. Elements released by oxidation and dissolution of primary ore minerals may be integrated into secondary minerals via precipitation, sorption or ion exchange (Jambour, 1994; Bernhard and Fontboté, 2001).

With a greater understanding of the chemical reactions and mineral transformations that are taking place within the tailings, coupled with the knowledge of the mineralogy and mineral chemistry of the primary ore, it is possible to determine the mobilisation of the elements throughout the tailings. This knowledge can then be transferred to other fields of study with interests in the mobilisation and fixation process of elements in near surface environments.

Geographical and geological setting

Mount Gunson is situated between 31°06'00"S and 32°00'00"S and between 136°45'00"E and 137° 30'00"E on the Torrens 1:250 000 sheet within the Stuart Shelf geological province. The Stuart Shelf province consists of a relatively thin mostly flat Mesoproterozoic to Neoproterozoic sedimentary cover sequence, resting on Mesoproterozoic to Palaeoproterozoic basement of the Gawler Craton (Preiss, 1987). A major northerly trending discontinuity known as the Torrens Hinge zone forms the eastern margin of the Stuart Shelf and Gawler Craton which is located about 60 km to the east of Mount Gunson (Figure 1) (Preiss, 1987; Tonkin & Creelman, 1990).

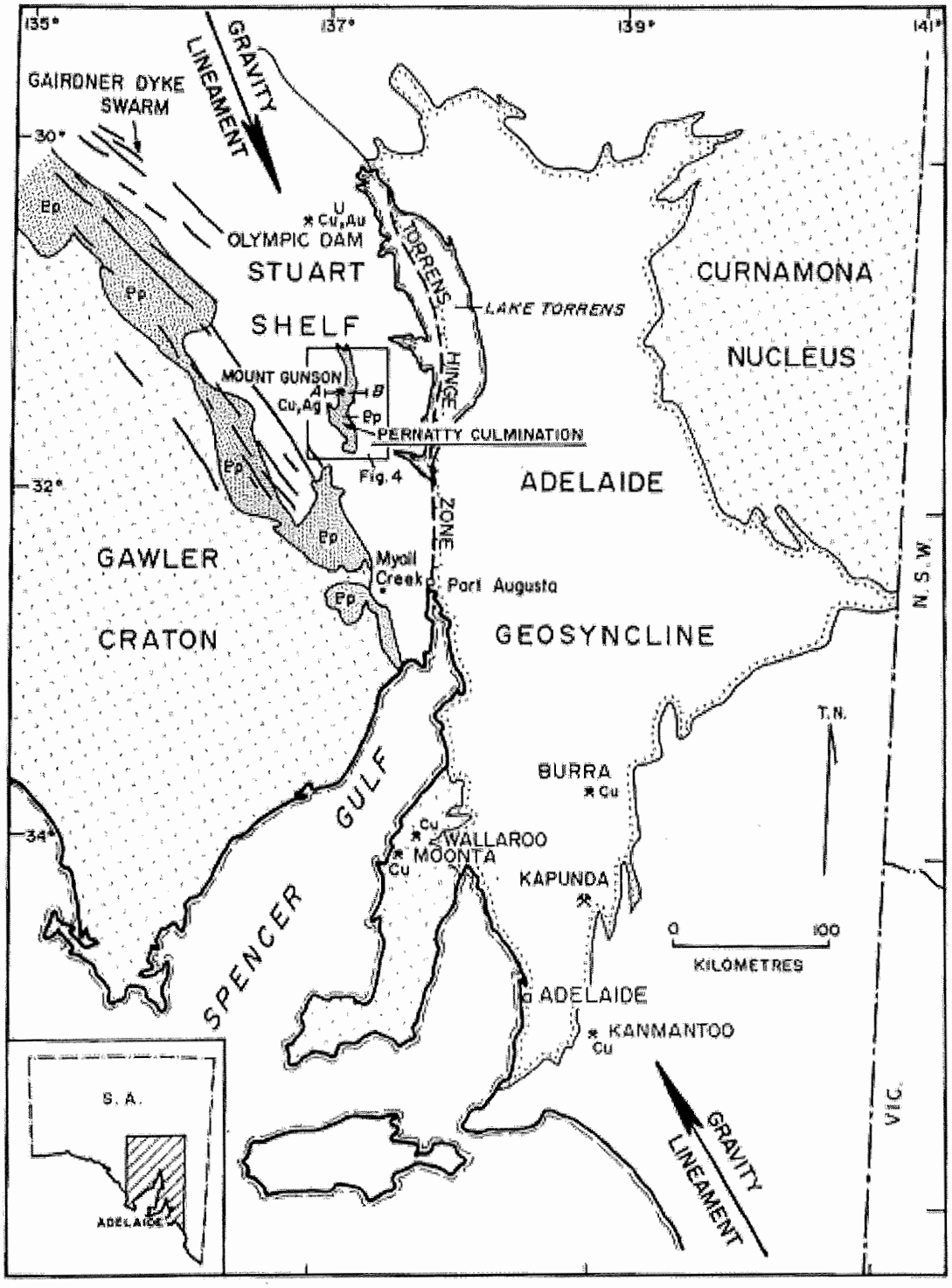

Figure 1. Location and regional geological setting of Mount Gunson (Tonkin & Creelman 1990).

The bedrock sequence in the area ranges in age from Paleoproterozoic to Neoproterozoic and is unconformably overlain by soil, sand dunes and salt lake deposits. The Pandurra Formation overlying the Gawler Craton Basement characterizes the sequence geology of the Mount Gunson region. Outcrop of this sequence is extensive to the west of Pernatty Lagoon where it occurs and is referred to as the Pernatty Culmination. The Culmination has been interpreted as an uplifted horst block that has formed a topographical high and is a major influence on the Neoproterozoic sedimentation (Figure 2) (Maiden, 1989). Faulting related to the uplift, permeable rock units and unconformity zones acted as conduits for mineralising fluids that formed copper deposits (Tonkin & Creelman, 1990). After a lengthy hiatus, a marine transgression unconformably deposited a sequence of Neoproterozoic sediments known as the Tapley Hill Formation and Whyalla Sandstone (Maiden, 1989).

Copper deposits

The Mount Gunson copper deposits are located in the Neoproterozic Stuart Shelf, overlying the eastern edge of the Gawler Craton, and are featured within the NNW trending transcontinental lineament known as the G2 corridor, which also extends through the Olympic Dam, Moonta and Wallaroo copper deposits (Preiss, 1987).

Mineralisation at Mount Gunson is closely related to porosity and permeability of the hosting lithologies, and occurs in regions where the stratum is most permeable and porous due to the depositional and/or erosional features of the Pernatty Culmination. There are two types of copper deposits at Mount Gunson, one being hosted in the black shale Tapley Hill Formation and the second a Sandstone breccia and sandstone hosted deposit in the Pandurra Formation and Whyalla Sanstone known as Cattle Grid (Solomon and Groves, 1994).

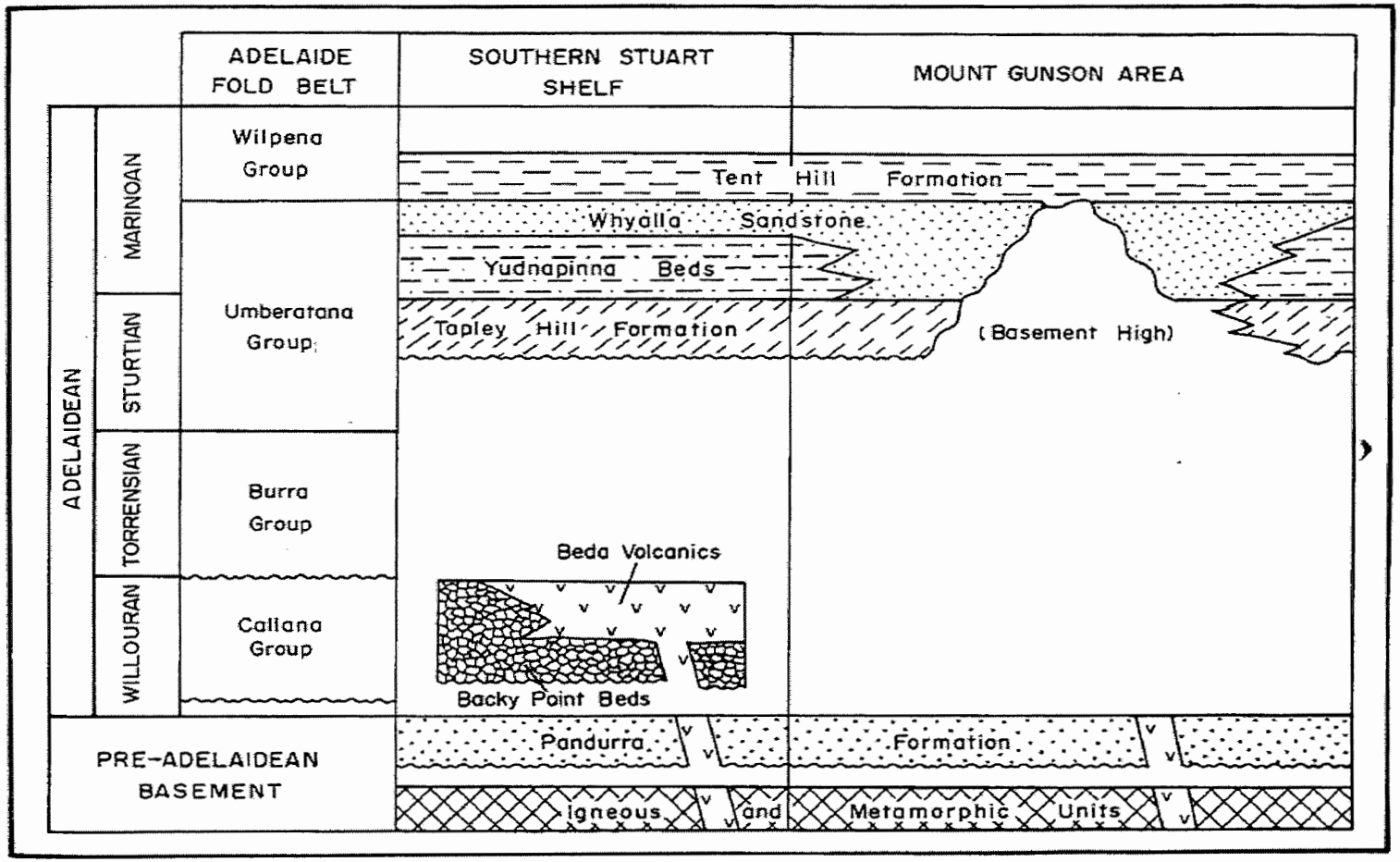

Figure 2. Southern Stuart Shelf and Mount Gunson stratigraphy, showing Pernatty Culmination in the Mount Gunson region (after Tonkin & Creelman 1990).

Cattle Grid

The Cattle Grid deposit is located on the western flank of a north-south trending ridge. Study by Lintern et al., (1998) has shown that the mineralisation (Figure 3) occurs at the interface between the brecciated upper surfaces of the Pandurra Formation, a medium to very coarse grained, poorly sorted, cross-bedded, red lithic sandstone, and the Whyalla Sandstone, a flat-lying medium to very coarse grained, moderately well sorted quarztose sandstone (Busbridge, 1981 unpublished). Sulphide mineralisation involved the replacement of pyrite and Cu-Fe sulphides by progressively more Cu-rich phases. The precipitation of the sulphide minerals predominantly infills fractures and vugs at and near the fossil surface due to oxidised cupriferous brines moving upward along faults and paleosurfaces associated with the Pernatty Culmination (Gersteling & Heape, 1975; Knuts et al., 1983; Lambert et al., 1987; Solomon & Groves, 1994).

The deposit consists of a complex sulphide mineral assemblage, which is dominated by the presence of chalcopyrite ($CuFeS_2$) – chalcocite (Cu_2S) – bornite (Cu_5FeS4). It also contains notable amounts of pyrite, sphalerite and carrollite, with minor amounts of Ag, Co, Zn, Pb, Ni, Bi, and traces of Au (Gersteling & Heape, 1975; Rattigan et al., 1988; Tonkin & Creelman, 1990). Concentrate assays from the deposit revealed a non – equilibrium mineral assemblage of chalcopyrite = < 35 % copper, bornite = 34 - 44 % copper and chalcocite => 44 % copper suggesting a mineral zoning. With a chalcopyrite zone to the northwest and rimmed on the southeast side by a bornite zone, which inturn is further rimmed by a chalcocite zone (Figure 4). The paragenesis of the Cattle Grid deposit is as follows pyrite-carrollite → chalcopyrite → bornite → chalcocite → sphalerite-galena (Tonkin and Creelman, 1990).

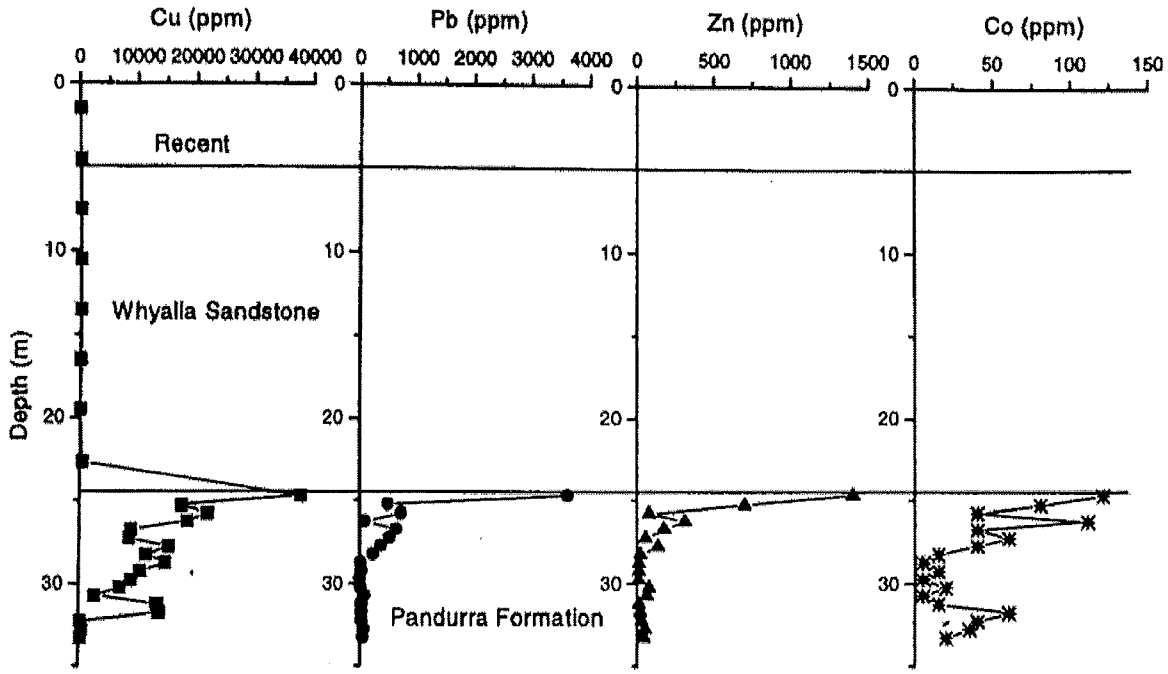

Figure 3. Geochemistry profile between the Whyalla Sandstone and Pandurra Formation (after Lintern et al., 1998).

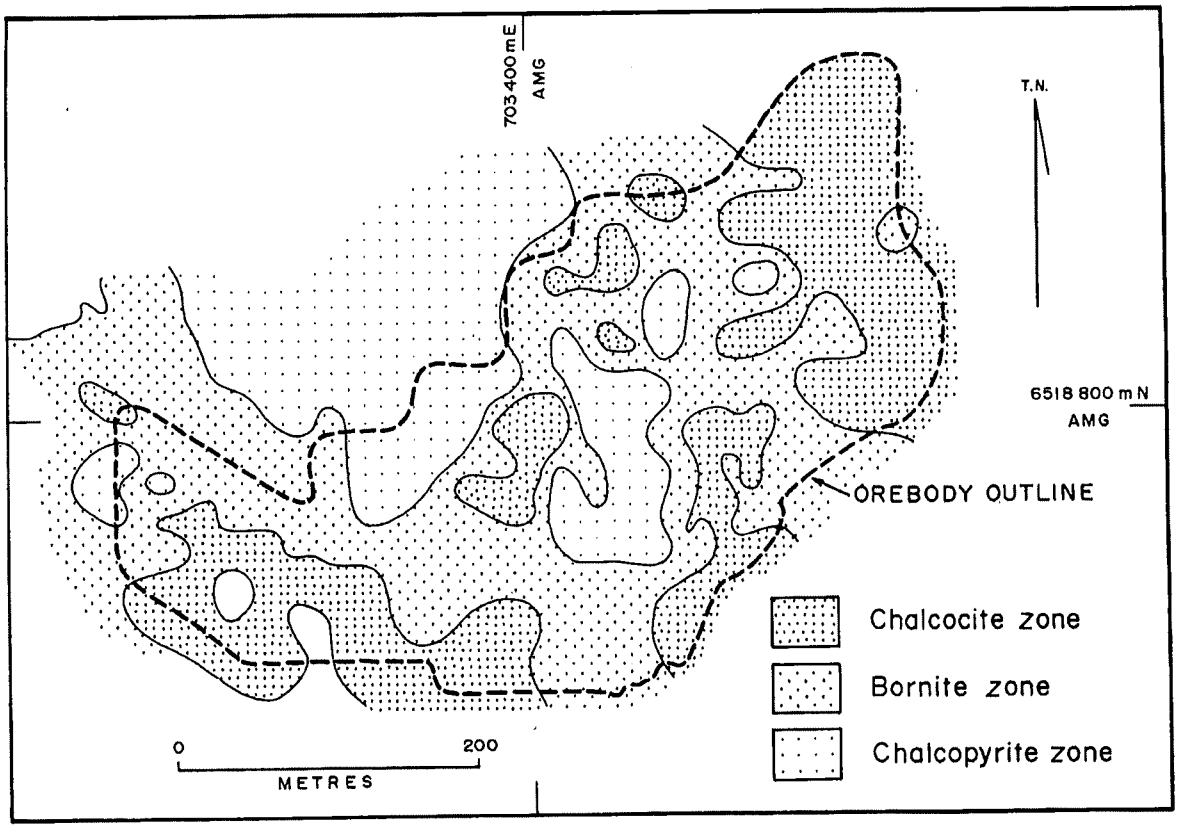

Figure 4. Mineralogical zoning of the Cattle Grid ore body, (after Tonkin and Creelman 1990).

Mining at cattle grid and the formation of the tailings

During 1974-1984 CRS (Crest Magnesium NL) with partners commenced mining. Recovery of the ore was achieved, initially by removing the overburden to within 1 m of the ore, using tractor scrapers and heavy bulldozers (Figure 5).

Once the ore was exposed, blasting (Figure 6) and the use of a Komatsu WA400 Front End Loaders trammed 2 m x 3 m blocks of ore to the feeder bins. This was followed by three crushing stages, interwoven with screening, grinding in the ball mill and separation according to size in the cyclone. All theses stages exist to reduce the ore to fine sand size of 330 microns so that the minerals are present as individual particles. Flotation is then used to separate the valuable copper from the ore. The flotation process takes place in flotation cells; chemicals xanthate and SF 323 (collectors) and teric 401(frother) are added. The chemicals xanthate and SF 323 are specially chosen, as they have the ability to form a link between the copper minerals and air bubbles. The copper minerals adhere to the air bubbles and rise to the surface. The addition of the flotation agent teric 401 forms a stable froth layer on the top of each cell. The rising air bubbles continually build up the froth layer, and the froth accumulation is allowed to flow off the top of each cell into a launder (Bradshaw 1984).

Figure 5. Removal of the overburden using heavy machinery (after CSR annual report 1974 – 1984).

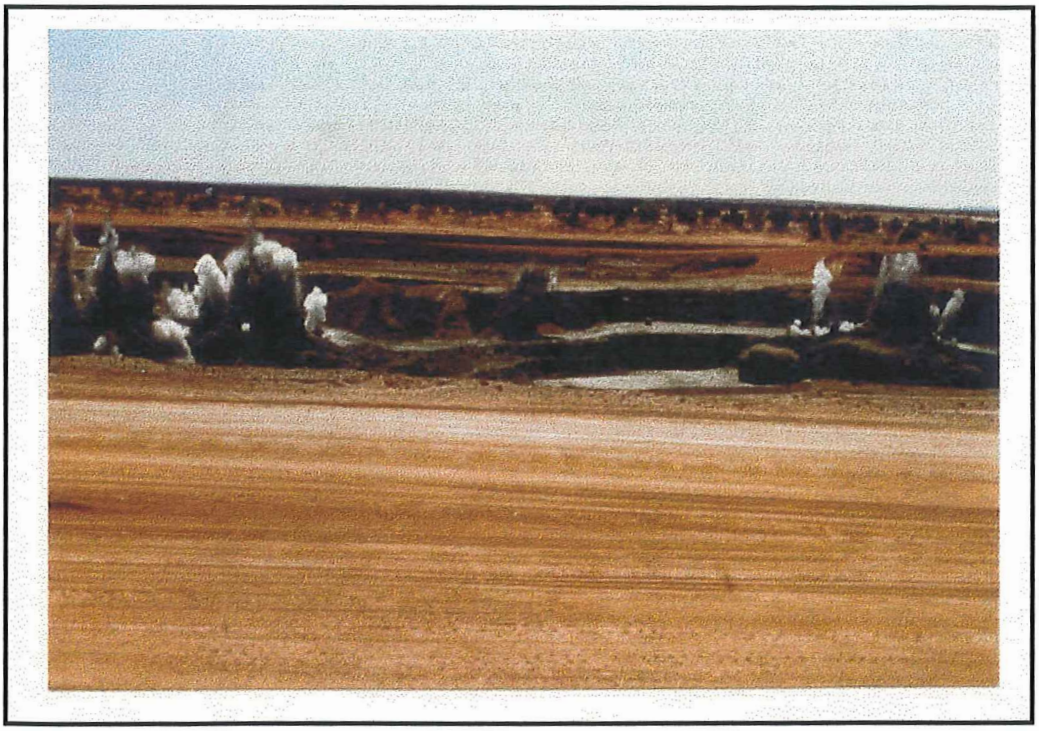

Figure 6. Blasting of the ore in the Cattle Grid open cut deposit (after CSR annual report 1974 – 1984).

The tailings from the flotation section were discharged to a thickener where flocculant was added. Clear overflow water was returned to the mill circuit and the thickened tailings were pumped to a tailings dam at a higher level than the plant, which enabled the reclamation of water (Houston, 1977; Harding, 1984). This venture resulted in the formation of 3 storage impoundments (dams 1, 2 and 3). The dams were constructed, as down-stream impoundments at 38^{O} to horizontal. The construction of the tailings dams was achieved with the cycloning of the coarser fraction of the tailings to form the embankment at the downstream side of the dam (Figure 7). Followed with the finer fraction being slurried to the upslope side of the dam, (Woodburn Fitzhardinge Geotechnical Consulting Engineers, 1987).

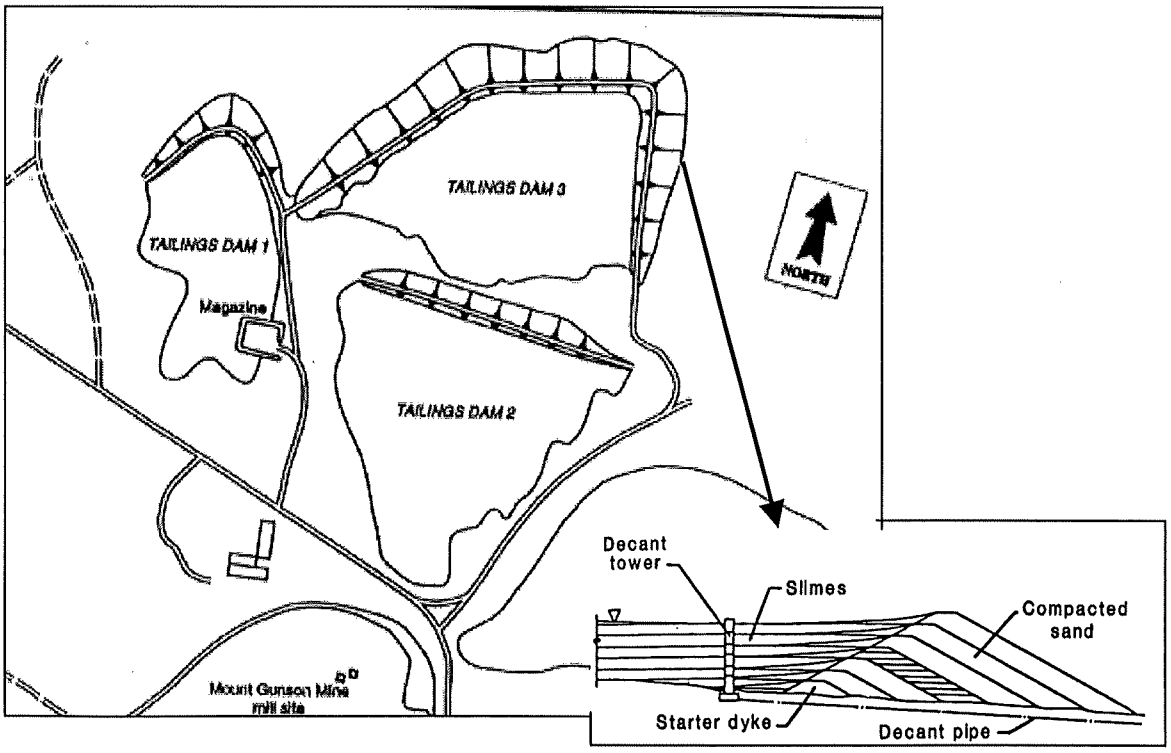

Figure 7. Outline of tailings dam with the downstream design for the outer embankments. Cross-section indicates the location of the coarse and fine fractions. (Modified from CRS operations manual 1974 – 1986).

The aim of this study is to investigate the mineralogical and geochemical changes within the three tailing impoundments. Impoundment (1) was commissioned between the years 1974-1976, impoundment (2) 1976-1980 and impoundment (3) 1980-1986. The Cattle Grid tailings deposit was chosen for the study, as extensive information about the origin of the tailings exists. This information includes the data on the host rock mineralogy, climate and flotation processes.

The host rock mineralogy consisted of > 95 % SiO_2 with very little micas and feldspar minerals (Puccini, 1996). The climate is classified as semi arid with relatively low precipitation rates 100 - 200 mm and high evaporation rates 2400 - 2500 mm (BOM, 2002). The flotation process and the knowledge that no other anthropogenic alterations had taken place after the tailings were decommissioned. The study focuses on the effects of pH, and fO_2 in reference to climate and rainfall, physical characteristics such as grainsize of the residual ore and gangue minerals that may influence the mobilisation and distribution of elements within the tailings.

Methodology

Sample collection

The Mount Gunson Tailings were visited during June / July 2002 for the purpose of sample collection. Locations for core samples to be taken were chosen according to the different ages of the tailings impoundments (1, 2 and 3) and the distinct grainsize distribution across the tailings. These locations (shown in Figure 8), are MGL 706736 (E) / 6520418 (N) outer edge of impoundment 1, MGF 7070729 (E) / 6520229 (N) outer edge of impoundment 2 and MGA 707332 (E) / 6520411 (N) outer edge, MGB 707187 (E) / 6520477 centre of impoundment 3.

Using (RKS) Percussion drilling equipment (Figure 9) vertical sequence to the depths of 8m (MGL), 10m (MGA), 7m (MGB) and 7m (MGF) were collected.

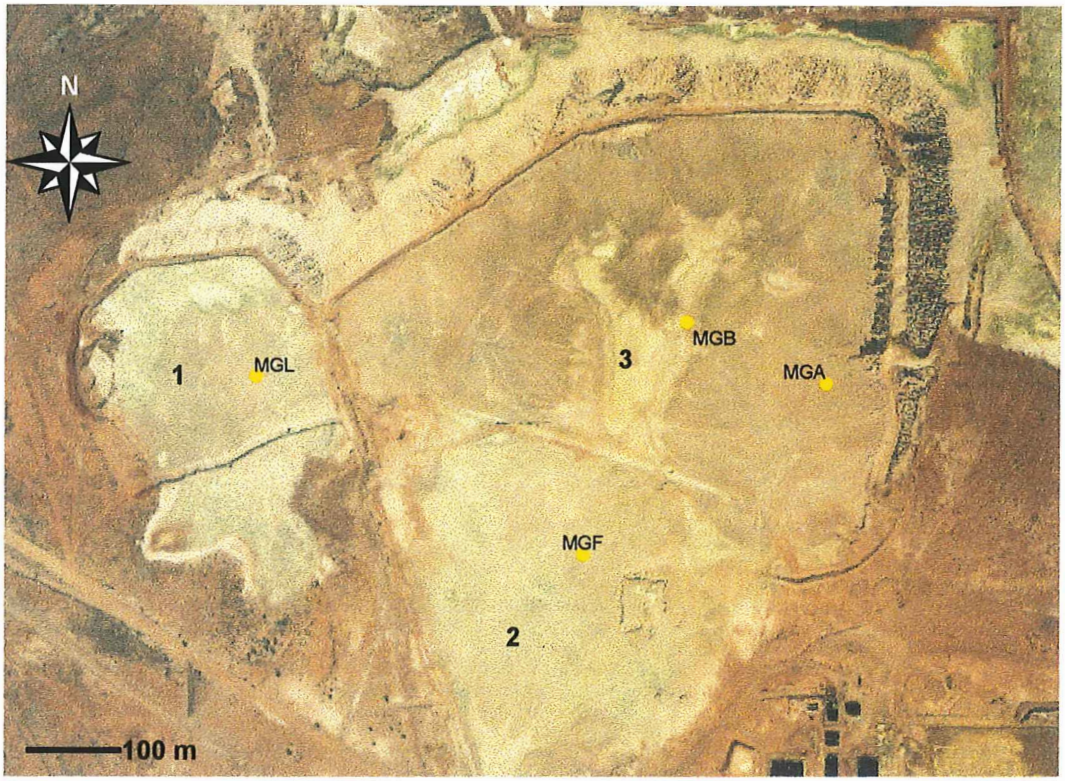

Figure 8. Aerial photo showing location of cores obtained, MGL (1), MGF (2), MGA and MGB (3)

Figure 9. RKS drilling equipment used to extract core from the three impoundments MGL, MGF, MGA and MGB.

The samples collected were subdivided into 1 m cores and logged visually for characteristics such as colour and grainsize. The pH was obtained via paste method (Inoculo soil pH test kit). Samples were then packaged in plastic resealable bags for transport back to Adelaide University. Using this approach 32 samples were obtained from the three impoundments, each representing a 1 m section of the representative drill core.

Regolith map

Aerial photo interpretations and groundtruthing were applied to produce a regolith map of the Mt Gunson tailings. Methods and procedures were adopted from the CRC LEME, Regolith mapping workshop Olary domain, field book and user guide, 2nd edition (Pain et al., 2000). The same landform definitions have been adopted and have been applied to the tailings. A regolith map was produced using ArcView v 3.2a software. The aim of the regolith map is to define correlations between landforms and elevated element concentrations.

Sample preparation

At the University of Adelaide laboratories, 100 g of each of the tailing samples were dried in watch glasses and the moisture content [wt %] determined. Once determined the samples were crushed to a fine powder, using a tungsten carbide crucible and ring grinder. The crushed fine powder was divided into two and analysis of major and trace elements was performed using XRF.

Major element

Small amounts of the powdered samples were transferred into alumina crucibles and ignited overnight in a furnace at 960^{O} C, to yield the loss on ignition (LOI) values.

One gram of the ignited material was then accurately weighed with 4 g of flux. The sample-flux mixture was fused using a propane-oxygen flame, at a temperature of ~ 1150^{O} C, using Pt - Au crucibles, and then cast into a preheated mould to produce a glass disc for analysis of major elements (SiO_2, Al_3O_3, MnO, CaO and Na_2O) using a Philips PW 1480 XRF Spectrometer

Trace elements

Approximately 5 - 10 g of powdered samples were mixed with 0.8 ml of binder solution (Poly Vinyl Alcohol) and pressed to form pellets. The samples were analysed using a Philips PW 1480 XRF Spectrometer.

From core MGL, samples from selected depths 125 - 150 cm, 219 - 275 cm, 325 - 375 cm, 425 - 475 cm and 625 - 725 cm were prepared for x-ray diffraction (XRD). Preparation required the separation of the heavy mineral fraction from the bulk sample and this was achieved by running the bulk sample over a Wilfley table. Once separated, a portion of the heavy mineral fraction was then mounted on glass slides for mineralogical analysis by x-ray diffraction (XRD), using a Philips diffractometer, fitted with a graphite crystal diffracted beam monochrometer CoKα radiation 50 kV, 35 mA. Each sample was scanned over a range $3\text{-}75^{0}$ at a speed of 2^{0} 2 θ per minute and data was collected at 0.05^{0} 2 θ intervals.

The remaining heavy mineral fraction was used to prepare into polished sections for optical examination and electron microprobe analysis. All polished sections were studied under a microscope to identify the heavy minerals present, and at what depths. The polished sections were then photographed in quarter section to produce a mosaic. This was to enable easy location of selected minerals at specific depths for microprobe analysis.

Results

Impoundment descriptions

Impoundment 1

Tailings in impoundment 1 were derived from mining of the Cattle Grid deposit during 1974 – 1976. The obtained 8 m core (MGL) exhibited a distinct upper region 0 - 1.20 m revealing well-defined sandy-golden horizons; with pH values ranging from 4.5 - 5.5. The lower region of the core 1.20 – 8 m was dominated by dark grey/green horizons with pH values ranging from 4.5 - 8 (Figure 10a). The core was dominated by an average grain size of 0.33 mm. (See appendix 1. for core descriptions).

Impoundment 2

Tailings in impoundment 2 were also derived from mining of the Cattle Grid deposit, during 1976 – 1980 The obtained 7 m core (MGF) showed a distinct upper region 0 -1.15 m revealing well-defined sandy-golden horizons, with pH values ranging from 5 – 5.5. The lower region 1.15 – 7.0 m was defined visually by distinct green/grey horizons, with pH values ranging from 5.5 – 7 (Figure 10b). The core was dominated by an average grainsize of 0.33 mm. (See appendix 1. for core descriptions).

Impoundment *3*

Tailings in impoundment 3 contained tailings from two different deposits, which were deposited during (1980 – 1986). The main deposit of tailings was derived from Cattle Grid, whilst in the upper north-eastern region of impoundment 3, tailings were derived from the Main open cut (MOC), where the principle ore mined was atacamite.

The two drill cores obtained from impoundment 3 revealed that the upper region 0 - 2 m (MGA = 0 - 1.99m and MGB = 0 - 1.74m) consisted of extensively thick sandy yellow horizons, with pH values ranging from (MGA = 4.5 - 6; MGB = 5.5 - 6) and a grain size of .33mm. The lower region (MGA = 1.99 - 10.0 m; MGB = 1.74 - 7.0 m) was defined visually by its dark green/grey horizons and pH values ranging from (MGA = 6 - 7; MGB = 6 - 7) (Figure 10 c & d) and had a grain size of 0.33 mm for MGA and 0.125 mm for MGB. (See appendix 1. for core descriptions).

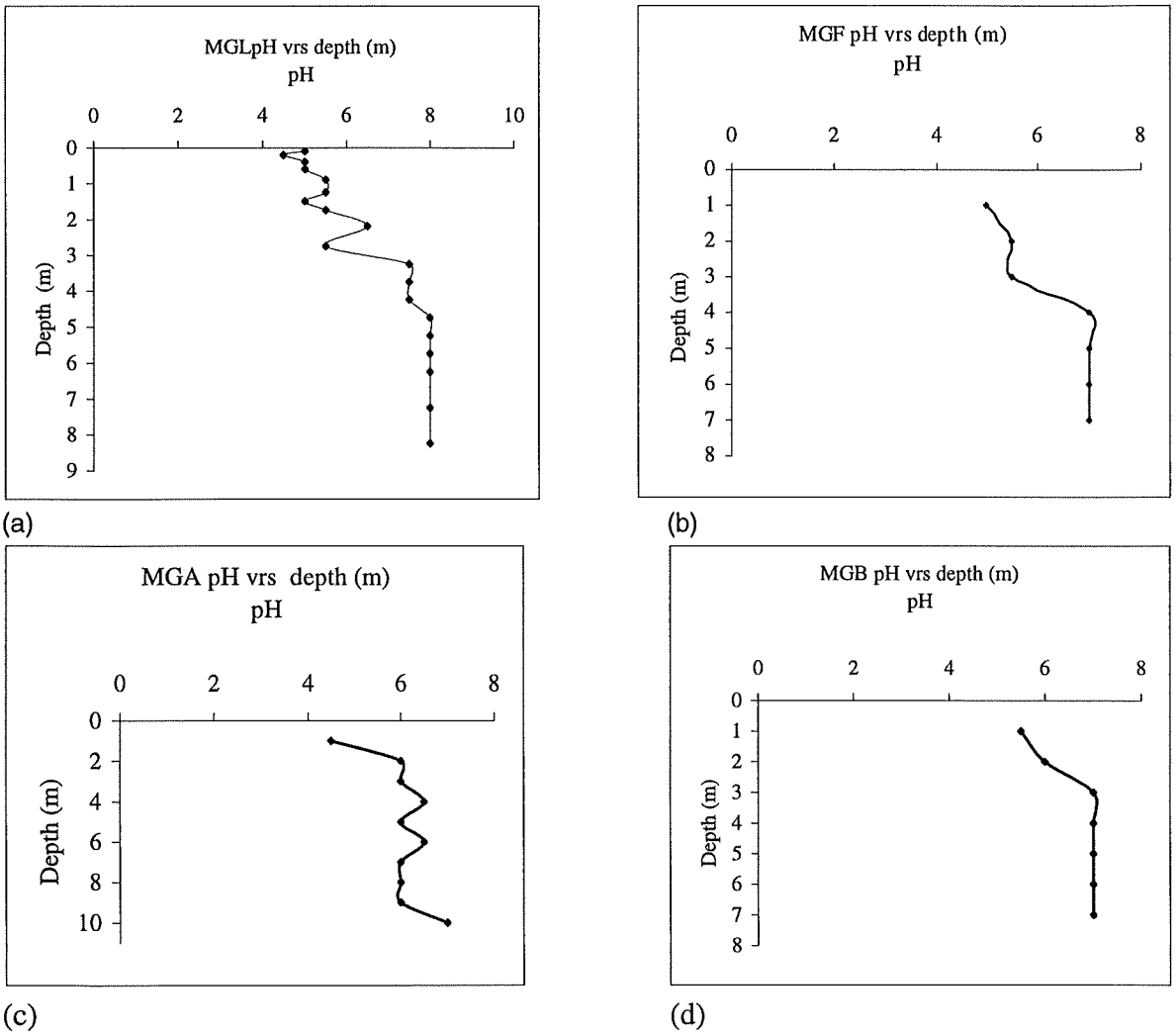

Figure 10. pH vrs depth (m) within the three tailings MGL (a), MGF (b), MGA (c) and MGB (d). Reveals that as depth increases pH increases.

Moisture content for the cores MGA and MGF ranged between 8 - 9 wt % and increased downward to 14 wt %. In contrast the central location of MGB revealed moisture contents ranging from 16 wt % and increased downward to 22 wt % (Figure 11 a - c). In view of the relatively low precipitation rates 100 - 200 mm and high evaporation rates 2400 - 2500 mm (Figure 12), the tailings are considered quite moist.

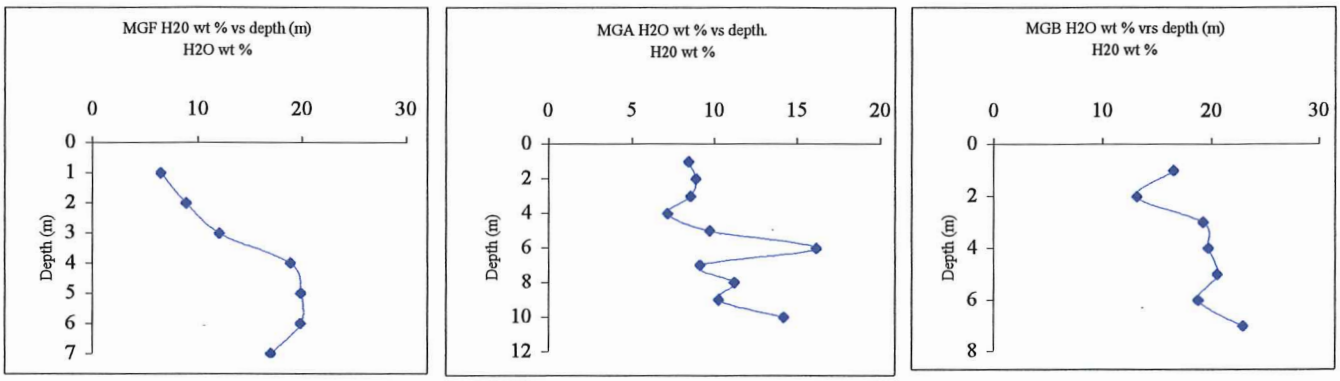

Figure 11. Illustrating moisture content throughout the tailings. (a) MGF, (b) MGA and (c) MGB

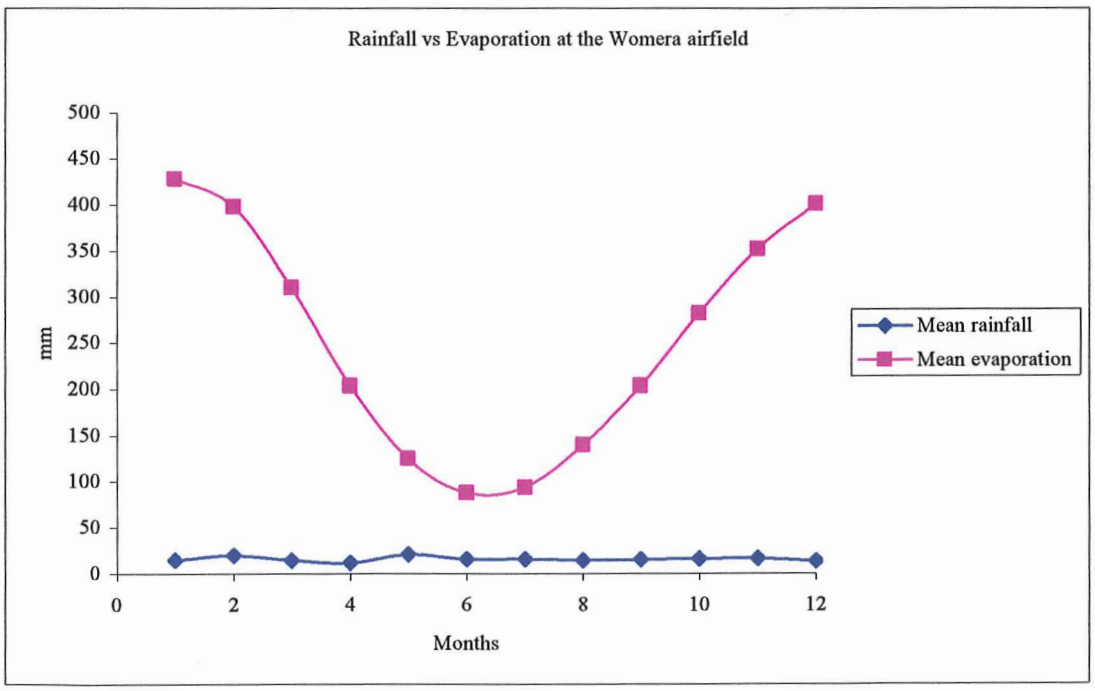

Figure 12 Precipitation and evaporation rates at the Woomera airfield 2002.

XRF whole rock analysis

XRF analysis revealed variation throughout the respective drill cores with the major element within the samples being SiO_2 with minor amounts of Al_2O_3 and Fe_2O_3. With high concentrations of trace elements Cu, Zn, Pb, Co and Ni that were noted to be in the tailings (Table 1.). Geochemical depth profiles of vertical sections through the upper 8 m show the distribution of these five elements (Figure 13 - 16). The concentration gradient within the three impoundments is Cu > Zn > Pb > Co > Ni.

Table 1. Displays major element %, and trace element concentration ppm from XRF.

Depth (m)	SiO_2 %	Al_2O_3 %	Fe_2O_3 %	Cu ppm	Zn ppm	Pb ppm	Co ppm	Ni ppm
0.1	89.33	4.73	0.61	848	213	47.2	493	22
0.2	93.64	3.37	0.52	447	136	42.1	239	11
0.4	89.12	4.12	0.58	726	200	74.8	236	15
0.6	88.15	6.62	0.62	966	154	80.0	306	18
0.9	87.93	5.57	0.56	967	184	116.7	263	23
1.25	85.32	7.26	0.88	2727	412	388.6	349	32
1.5	84.30	8.27	0.73	1666	306	90.6	242	23
1.75	86.71	7.20	0.85	2574	471	415.6	381	31
2.19	84.01	7.81	1.02	2951	674	309.7	486	36
2.75	89.23	5.38	0.80	1348	725	216.0	273	23
3.25	88.61	5.35	0.77	1502	830	279.1	199	18
3.75	87.83	5.40	0.75	2039	673	260.9	144	14
4.25	88.43	5.69	0.69	1169	502	225.5	204	17
4.75	81.76	9.84	0.91	1590	681	373.2	182	18
5.25	87.26	6.69	0.68	1527	532	237.7	132	15
5.75	85.11	7.15	0.77	3075	979	399.8	64	12
6.25	88.06	6.11	0.69	1939	625	260.8	90	11
7.25	88.10	6.14	0.72	993	412	167.5	189	19
8.25	88.65	5.72	0.70	1822	542	236.2	108	12

(See appendix 2 for all raw data).

Analysis of the drill core MGL from impoundment 1 (Figure 13) revealed that copper, zinc and lead display similar trends of fluctuation for increased and decreased concentrations throughout the 8 m core. High concentrations for Cu, Zn and Pb within the core are noticed at the 1 – 2 m section and 5 – 6 m section. Values recorded for the 2 m region were Cu = 2397 ppm, Zn = 483 ppm and Pb = 272 ppm and in the 6 m region Cu = 2507 ppm,

Zn = 802 ppm and Pb = 330 ppm. Low concentrations are located at the 7 m region with average concentration values of Cu = 993 ppm, Zn = 412 ppm and Pb = 167 ppm. As for elements Co and Ni they show increased concentrations at the 2 m region, with values of Co = 369 ppm and Ni = 30 ppm. As depth increases, 2 – 8 m there is a decrease in concentration with average concentration values of Co = 77 ppm and Ni = 15 ppm.

Analysis of the drill core sample from MGF at impoundment 2 (Figure 14) shows decreasing Cu concentration to depth. The highest recorded concentration for Copper was in the 0 – 2 m region with a value of Cu = 2139 ppm. With the lowest concentration of Cu = 717 ppm being recorded at the 5 m region. In contrast elements Zn, Pb, and Co throughout the 0 – 7 m remain relatively constant and show average concentrations of Zn = 255 ppm, Pb = 188 ppm, and Co = 219 ppm. Nickel remains relatively constant with an average concentration of Ni = 18 ppm in the upper 4 m and lower 6 – 7 m, but at the 5 m region there is an increase to 75 ppm.

Analysis of the drill cores from Impoundment 3, MGA and MGB (Figure 15 – 16) represent two regions and will be looked at separately. Drill core MGA (outer rim) shows similar fluctuation trends for copper, zinc and lead of variation throughout the 10 m core. High concentrations for Cu, Zn and Pb within the core are noticed at the 2 m, and 4 m region with recorded values for the 1 - 2 m region of Cu = 1879 ppm , Zn = 356 ppm and Pb = 214 ppm and in the 3 - 4 m region Cu = 1412 ppm, Zn = 284 ppm and Pb = 130 ppm. With the lowest concentrations of Cu = 630 ppm being recorded at the 10 m region, Zn = 86 ppm at the 5 m region and Pb = 90 ppm at the 2 - 3 m region. For the elements Co and Ni concentration values remain relatively constant throughout the core with an average concentration of Co = 120 ppm and Ni = 14 ppm.

In MGB (centre of impoundment) showed that the overall trend for copper is a decrease in concentration as depth increases with the highest concentration of Cu 2564 ppm recorded at the 0 - 1 m region and the lowest concentration of Cu = 778 ppm recorded at the 9 - 10 m region. As for elements Zn, Pb, Co and Ni their concentrations remain relatively static with average concentrations of Zn = 219 ppm, Pb = 207 ppm, Co = 131 ppm and Ni = 17 ppm.

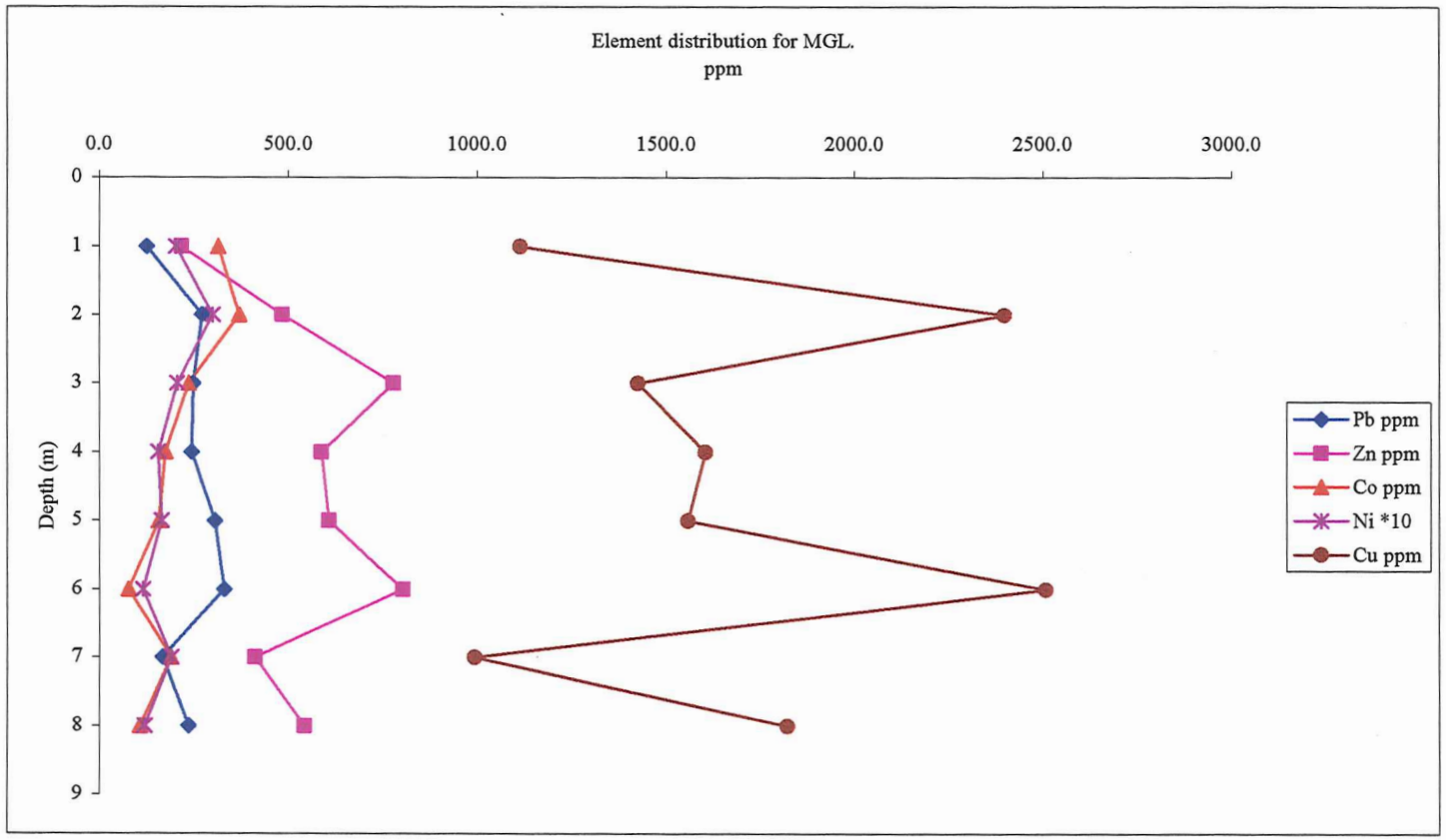

Figure 13. Geochemical profile for element distribution through impoundment 1 MGL. Concentrations at depths represent the bulk sample for that 1 m core (eg: Cu 1113 ppm is concentration for the depth O – 1 m). Note: Ni has been multiplied by 10 for observation purposes.

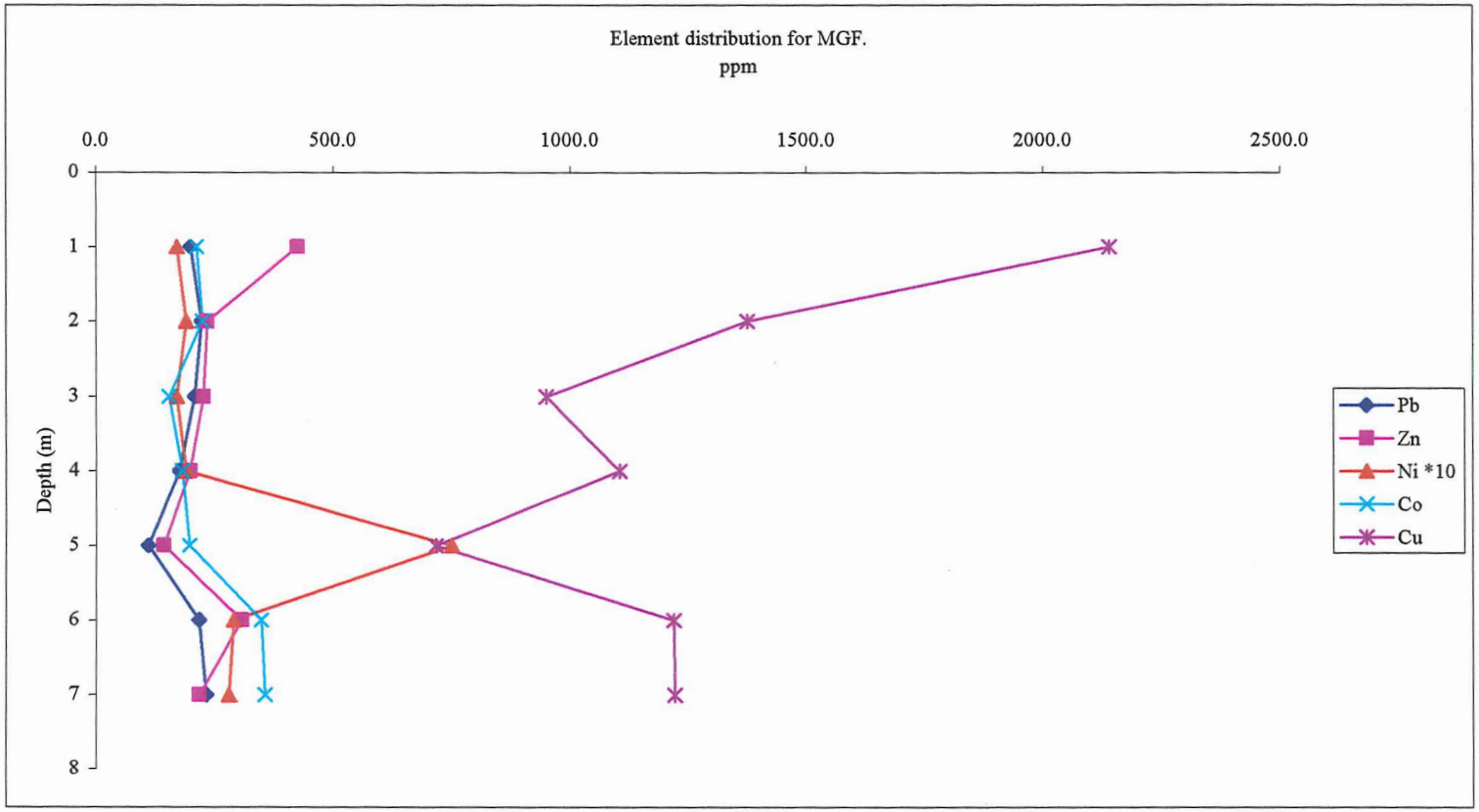

Figure.14 Geochemical profile for element distribution through impoundment 2 inner rim MGF. Concentrations at depths represent the bulk sample for that 1 m core (eg: Cu 2139 ppm is concentration for the depth O – 1 m). Note: Ni has been multiplied by 10 for observation purposes.

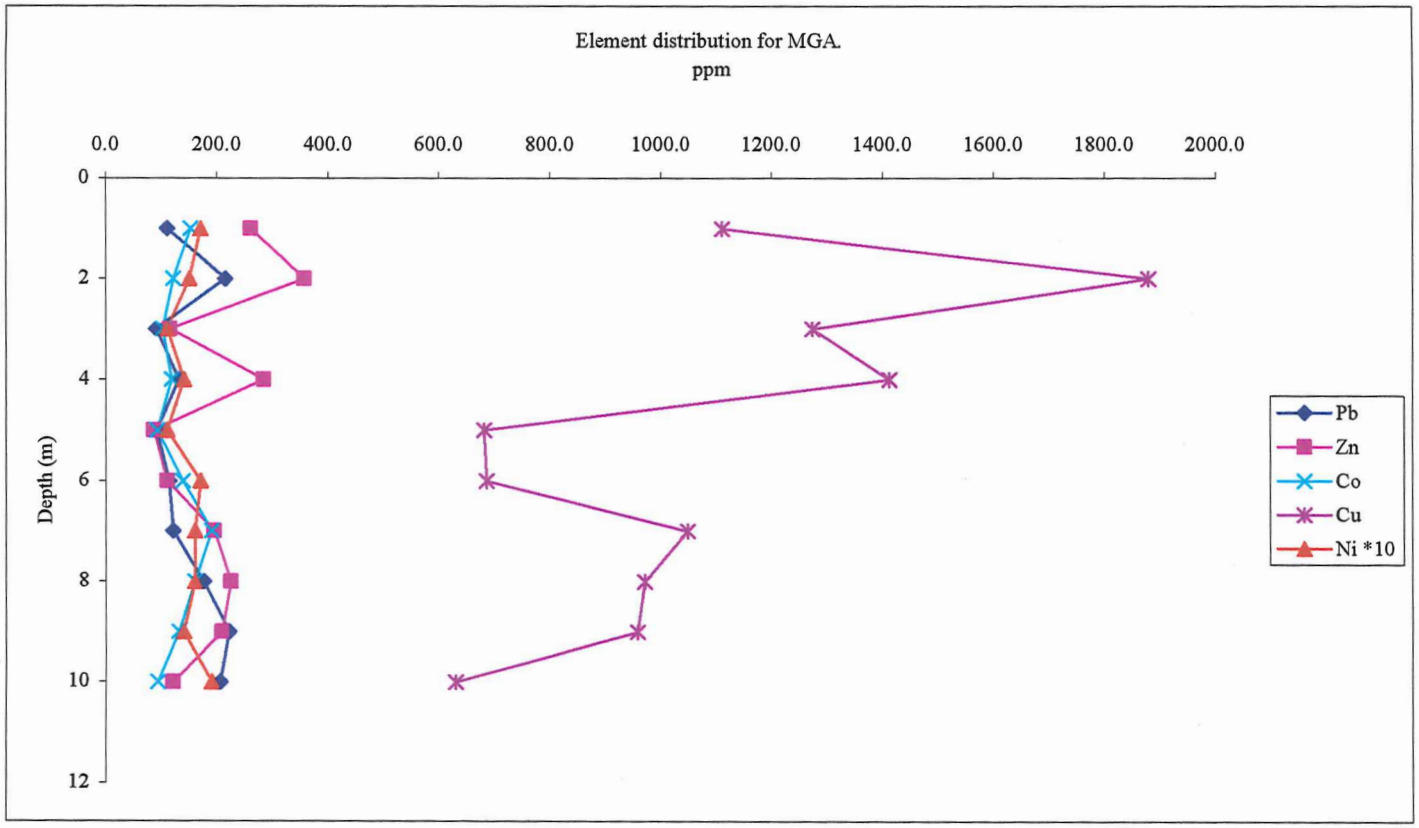

Figure15. Geochemical profile for element distribution through impoundment 3 outer rim MGA. Concentrations at depths represent the bulk sample for that 1 m core (eg: Cu 1110 ppm is concentration for the depth O – 1 m). Note: Ni has been multiplied by 10 for observation purposes.

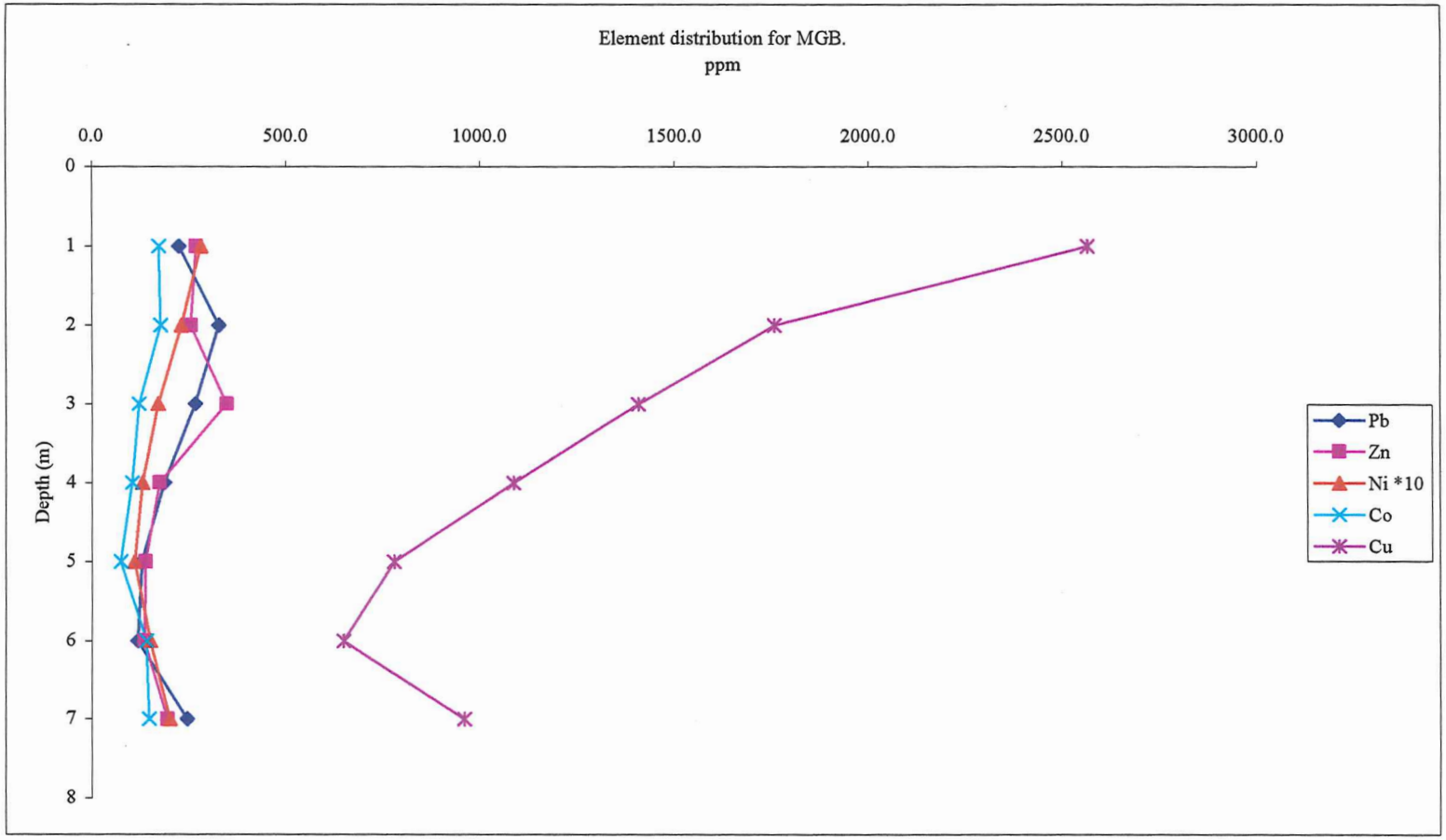

Figure 16. Geochemical profile for element distribution through impoundment 3 inner rim MGB. Concentrations at depths represent the bulk sample for that 1 m core (eg: Cu 2564 ppm is concentration for the depth O – 1 m). Note: Ni has been multiplied by 10 for observation purposes.

XRD and XRF major element analysis

XRD and XRF major element analysis confirmed that the tailings are dominated by primary quartz, with trace amounts of mica (muscovite) and kaolinite. The tailings thus directly reflect the composition of the ore, consisting of very pure Pandurra and Whyalla sandstone. The dominance of quartz throughout the profile and limitations of the XRD analysis made the identification of primary minerals such as chalcocite (Cu), bornite (Cu>Fe), chalcopyrite (Cu=Fe), pyrite (Fe), sphalerite (Zn), and carrollite (Co) difficult. Identification of primary minerals was only achieved by optical microscope studies coupled with electron microprobe analysis on heavy mineral concentrates.

Table 2: XRD results showing the overall dominance of SiO_2 (quartz)

Depth (cm)	Description	Quartz SiO_2	Muscovite $KAl_2(Si_3Al)O_{10}(OH,F)_2$	Kaolinite $Al_2Si_2O_5(OH)_4$
125 - 150	Oxidised	++++	+	++
219 – 275	Oxidised	++++	+	
325 – 375	Unoxidised	++++	++	
425 - 475	Unoxidised	++++		
625 - 675	Unoxidised	++++		

++++ very common mineral, +++ common mineral, ++ minor mineral, + trace mineral

Optical mineralogy

Petrographic analysis for core MGL showed that within the tailings, primary sulphide minerals pyrite, chalcopyrite, bornite, sphalerite and galena are present as finely crushed fragments.

In the upper 0 – 2 m all of the above minerals displayed signs of corrosion on their outer surface (Figure 17). The only significant difference was the degree to which they appeared corroded. Degrees of reactivity in the upper 0 – 2 m appeared to be sphalerite – galena > bornite > chalcopyrite> pyrite.

resulting in the skeletal fragments observed. Pyrite was predominantly observed with highly fractured outer edges showing signs of corrosion (Figure 17). Chalcopyrite and bornite showed differing degrees of corrosion. Chalcopyrite only appeared to show marginal signs of corrosion on its outer surface, while bornite showed evidence of enhanced degrees of corrosion (Figure 18a & b).

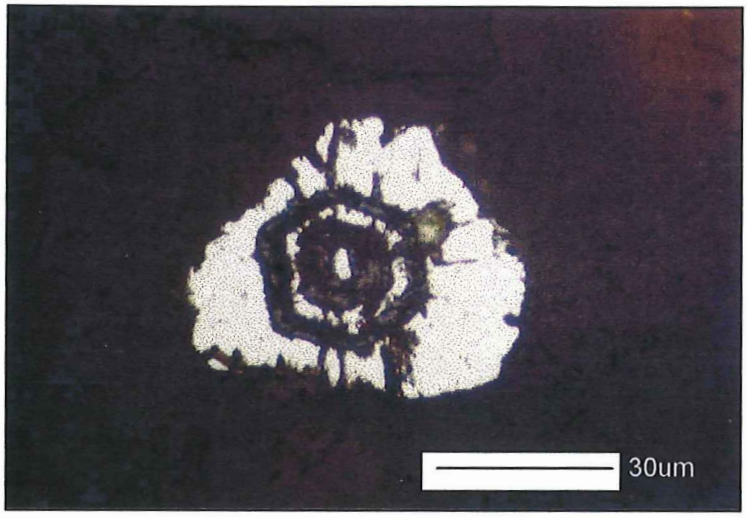

Figure 17. Pyrite grain displaying highly fractured corroded surfaces in the upper 2 m.

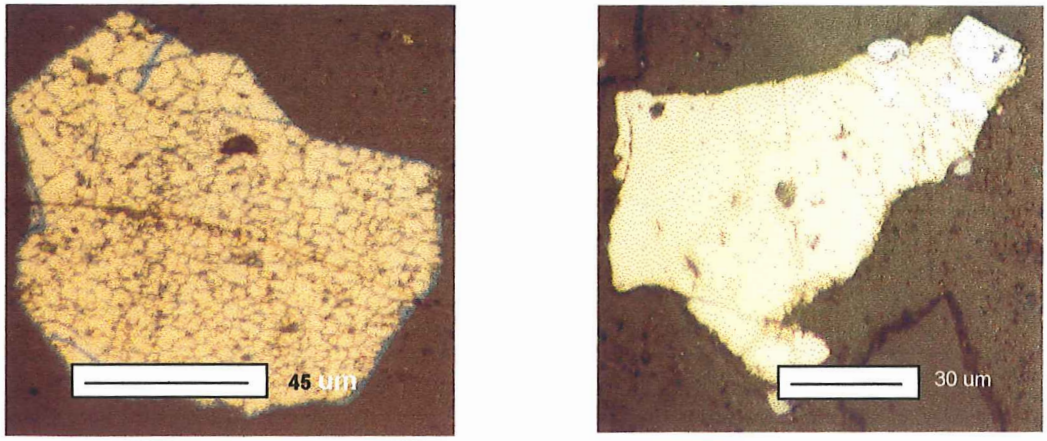

(a) (b)

Figure 18. Variable degrees of corrosion between bornite and chalcopyrite in the upper 2 m. (a) bornite, (b) chalcopyrite.

At depths below 2 m all of the sulphides appeared fresh showing very little corrosion on the surface. (Figure 19a - d).

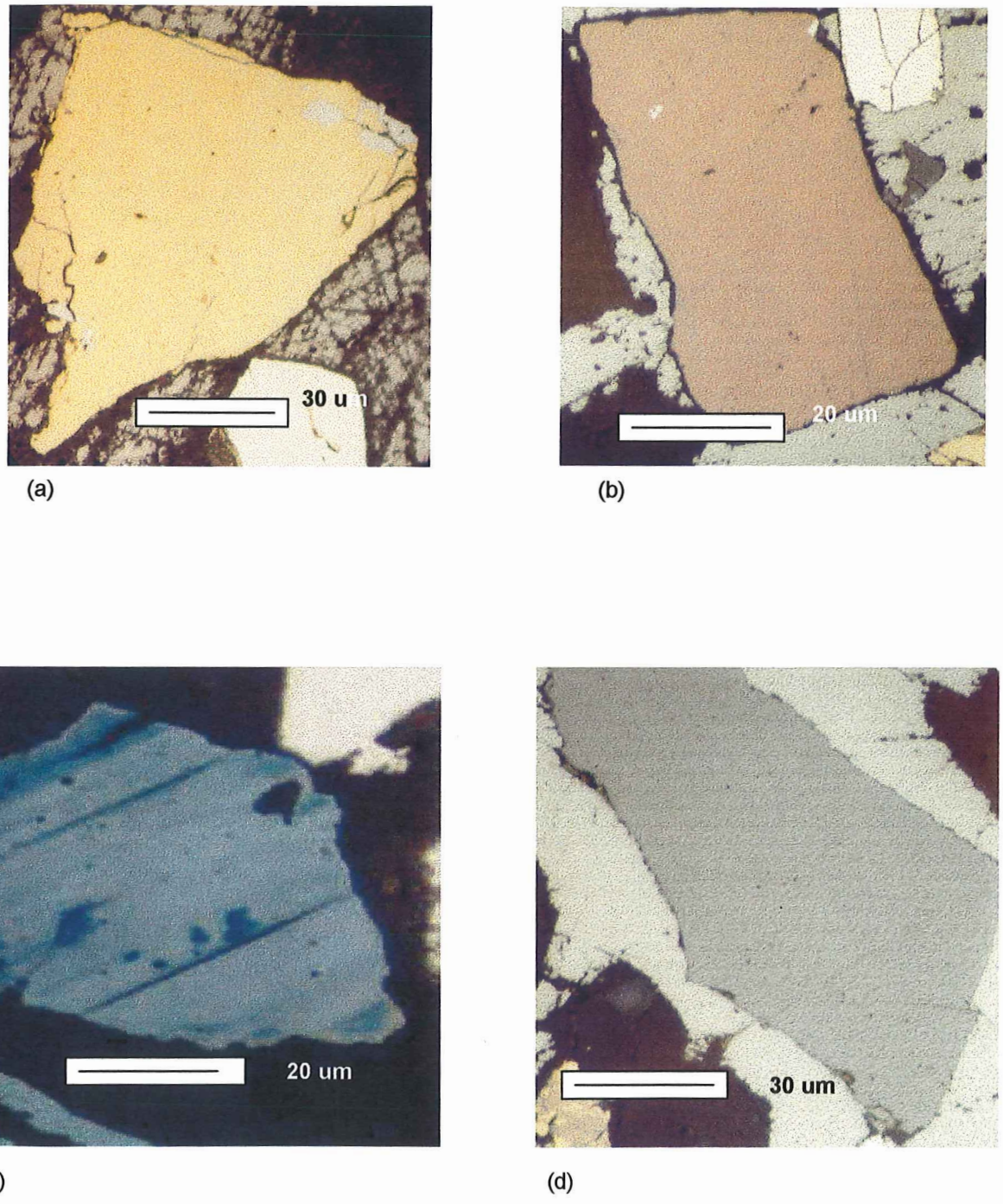

Figure 19. Primary sulphides at depths below 2 m revealing well defined edges free from corrosion. (a) chalcopyrite, (b) bornite, (c) covellite and (d) sphalerite.

What was clearly evident throughout the polished sections was the fluctuation in abundance of the sulphide minerals. At 0 – 2.75 m the dominant sulphide mineral was pyrite with small amounts of chalcopyrite, bornite and relatively rare fragments of sphalerite, galena and covellite. At 3.25 – 3.75 m the dominant sulphide is pyrite. Observations revealed that the content of copper bearing minerals is dominated by the mineral bornite. This was predominantly observed as finely crushed individual fragments, with the exception of one fragment, which displayed alternating layers of bornite and chalcopyrite on a micrometer scale (Figure 20).

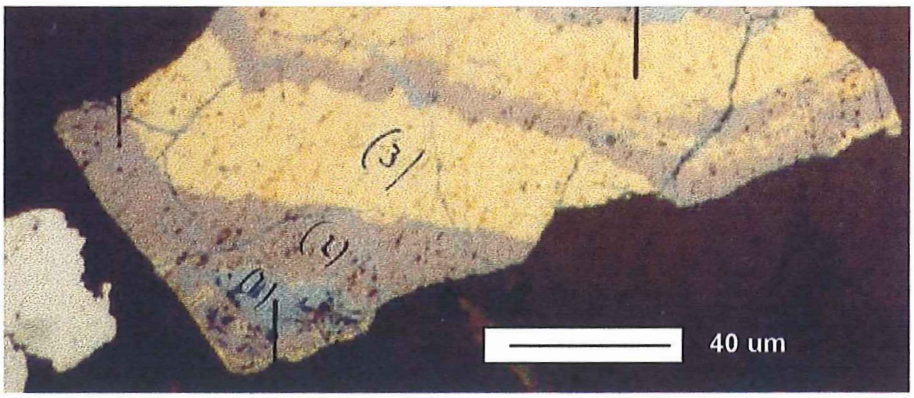

Figure 20. Bornite displaying alternating layers with chalcopyrite and small patches of covellite at a micrometer scale. (1) covellite, (2) bornite and (3) chalcopyrite.

Chalcopyrite was predominantly observed as fragments, and as fine growth bands within bornite. Covellite content increased to depth and is present as individual grains. Sphalerite and galena are observed as very fine (10 – 20 um) fragments. At the depth of 4.25 – 4.75 m chalcopyrite appears to be the dominant sulphide mineral when compared to bornite, with pyrite, sphalerite, galena and covellite being observed as relic fragments.

At 6.25 – 7.25 m chalcopyrite and bornite concentrations are similar with no one mineral appearing to dominate. Sphalerite, galena, pyrite and covellite grains are still recognised as individual fragments but their concentration is low.

Electron Microprobe analysis

Electron microprobe analysis was used to determine composition and trace element content in the respective sulphide minerals (pyrite, chalcopyrite, bornite, covellite and chalcocite) (Table 3). Major elements identified are copper and iron, with cobalt and nickel as trace elements. Concentration boundaries for the assigned copper fields of chalcopyrite 34.63 % Cu, bornite 63.31 % Cu, covellite 66.46 % Cu and chalcocite 79.85 % Cu (Deer et al., 1992). The element iron is rarely seen as a trace element. It is predominantly as a component of the minerals pyrite (FeS), chalcopyrite ($CuFeS_2$) and bornite (Cu_5FeS_4) (Figure 21 a). Zinc appears predominantly as trace amounts within chalcopyrite, bornite and covellite with values ranging between 0.1 – 1 [wt %]. Zinc content of 1 – 5 [wt %] in the copper sulphides suggest that zinc is possibly present as micro-inclusions, while values greater than 70 [wt %] correlate with the stoichiometric composition of sphalerite ZnS (Figure 21 b). Cobalt and nickel are present as trace elements with values ranging between 0 .1 - 1 [wt%] in pyrite, chalcopyrite, bornite and covellite. Some elevated values of 10 – 50 [wt%] cobalt and 1 – 10 [wt %] nickel, are related to the mineral carrollite $CuCo_{1.5}Ni_{0.5}S_4$ (Figure 21 c).

Table 3: Sample of probe analysis data for tailings mineral identification. From core MGL, samples from selected depths 125 - 150 cm (MGL 07), 219 - 275 cm (MGL 10), 325 - 375 cm (MGL 12), 425 – 475 cm (MGL 14) and 725 – 825 cm (MGL 18).

Sample #	W%(S)	W%(Fe)	W%(Co)	W%(Ni)	W%(Cu)	W%(Zn)	Total	Mineral
MGL 14 sample 4	50.0386	43.9599	0.0001	0.0597	1.6541	1.7793	97.4917	Pyrite
MGL 07 sample 1	50.1718	44.6373	0.3197	0.0659	1.0511	0.0084	96.2542	Pyrite
MGL 12 sample 3	49.699	44.958	0.0118	0.0579	0.2058	0.0001	94.9326	Pyrite
MGL 14 sample 6	25.8141	9.0962	0.0294	0.0001	67.4844	0.0651	102.4893	Bornite
MGL 12 sample 3	30.751	1.2792	0.0001	0.0001	70.1716	0.0001	102.2021	Covellite
MGL 07 sample 3	25.4221	10.7874	0.0001	0.0216	63.8688	0.0001	100.1001	Covellite
MGL 18 sample 5	32.6177	25.2401	0.0001	0.0267	43.9694	0.0001	101.8541	Chalcopyrite
MGL 10 sample 4	33.6101	28.7858	0.0309	0.0001	35.7373	0.0001	98.1643	Chalcopyrite
MGL 07 sample 4	34.0942	28.3358	0.9605	0.0555	34.628	0.049	98.123	Chalcopyrite
MGL 14 sample 9	33.6944	29.5942	0.0001	0.0172	34.6752	0.1347	98.1158	Chalcopyrite
MGL 12 Sample 5	41.1112	1.1883	23.2263	3.6919	22.1124	0.0001	91.3302	Carrolite
MGL 18 sample 4	40.9453	0.5956	25.2929	4.2537	18.9519	0.3033	90.3427	Carrolite
MGL 14 sample 4	31.8955	0.513	0.0001	0.0655	0.5666	66.004	99.0447	Sphalerite
MGL 10 sample 2	32.146	0.2632	0.0448	0.0735	0.5435	65.2544	98.3254	Sphalerite
MGL 10 sample 3	32.5762	0.1977	0.0116	0.0041	0.3873	64.6495	97.8264	Sphalerite

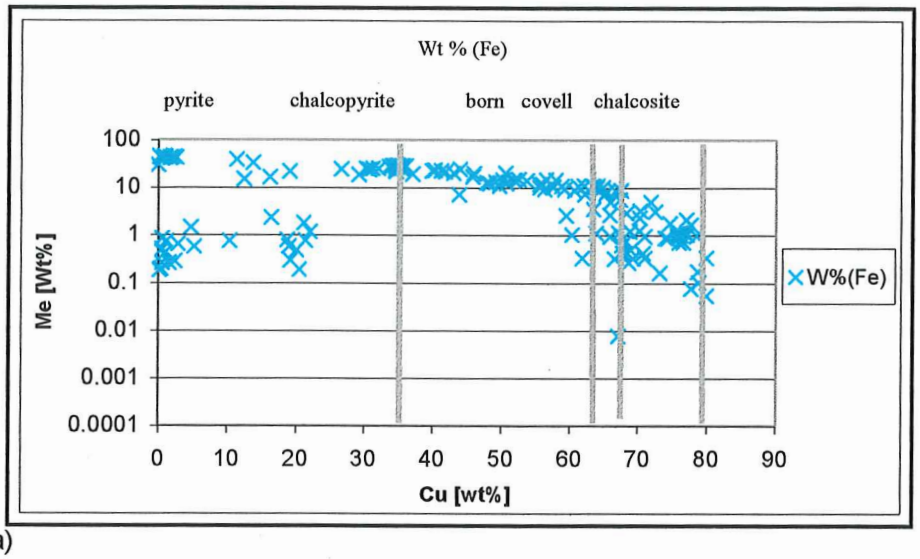

(a)

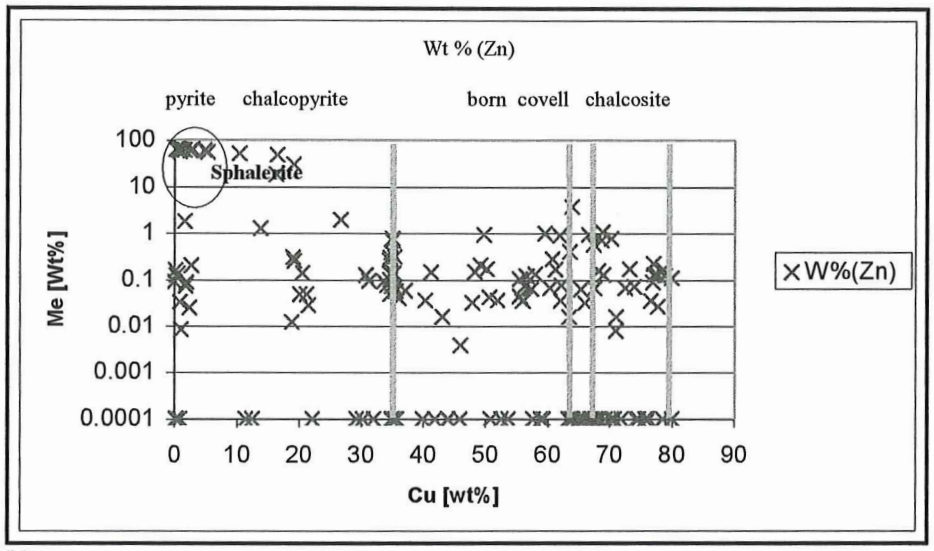

(b)

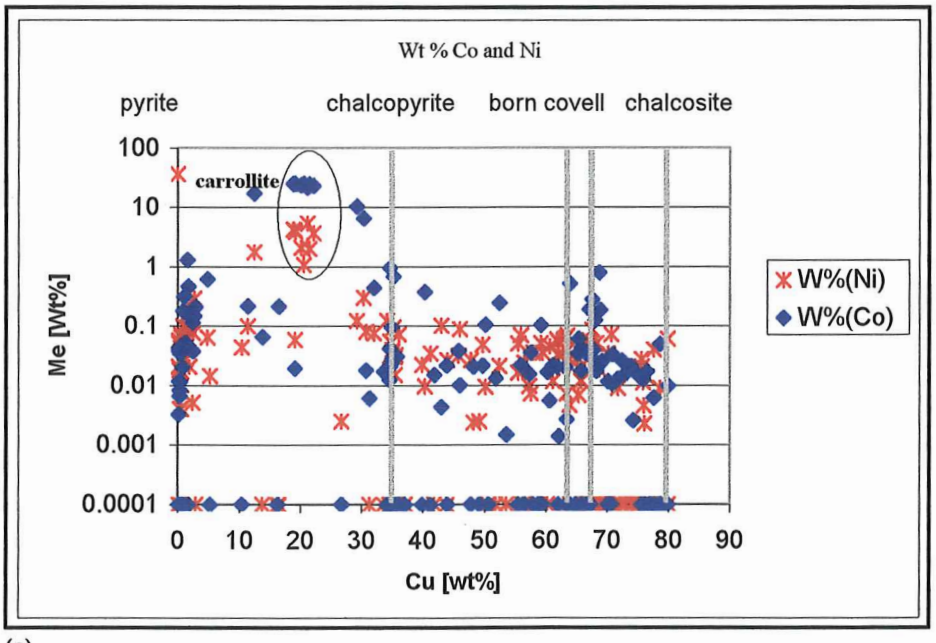

(c)

Figure 21. Copper boundaries and the relationship of compositional variation of the ore minerals in the tailings. (a) iron (b) zinc and (c) cobalt & nickel.

Discussion

Mass depletion

Losses or gains during weathering can be determined by comparing the average composition of the sandy yellow horizons (oxidised zone) and the dark green/grey horizons (reduced zone) (Table 4). The assumption is made that Zr is immobile as it resides mainly in the very stable mineral zircon. Based on this, equation (1) was suggested by (Holmström et al., 1999) to relate chemically mobile elements to the relatively stable Zr. From equation 1 shown, it is suggested that Zr is an immobile element and resides in minerals that are resistant to weathering (eg zircon). This is used to demonstrate weathering effects in the different tailings horizons, by plotting the average composition of the sandy yellow horizons (oxidised zone) with the composition of the dark green/grey horizons (Figure. 22).

Table 4. Average concentration of oxidised and unoxidised tailings at Mount Gunson, impoundment 1.

Element	OXIDISED TAILING		UNOXIDISED TAILING	
	Weight %	+/- std	Weight %	+/- std
SiO_2 %	87.61	+/- 3.00	87.30	+/- 2.25
Al_2O_3 %	6.11	+/- 1.73	6.35	+/- 1.36
Fe_2O_3 %	0.71	+/- 0.17	0.75	+/- 0.07
MnO %	0.00	+/- 0.00	0.00	+/- 0.00
MgO %	0.23	+/- 0.06	0.22	+/- 0.05
CaO %	0.04	+/- 0.02	0.05	+/- 0.02
Na_2O %	0.32	+/- 0.09	0.22	+/- 0.12
K_2O %	1.26	+/- 0.39	1.27	+/- 0.28
TiO_2 %	0.22	+/- 0.03	0.21	+/- 0.02
P_2O_5 %	0.06	+/- 0.01	0.06	+/- 0.01
SO_3 %	0.05	+/- 0.03	0.04	+/- 0.03
Zr ppm	182.4	+/- 13.1	173.4	+/- 7.7

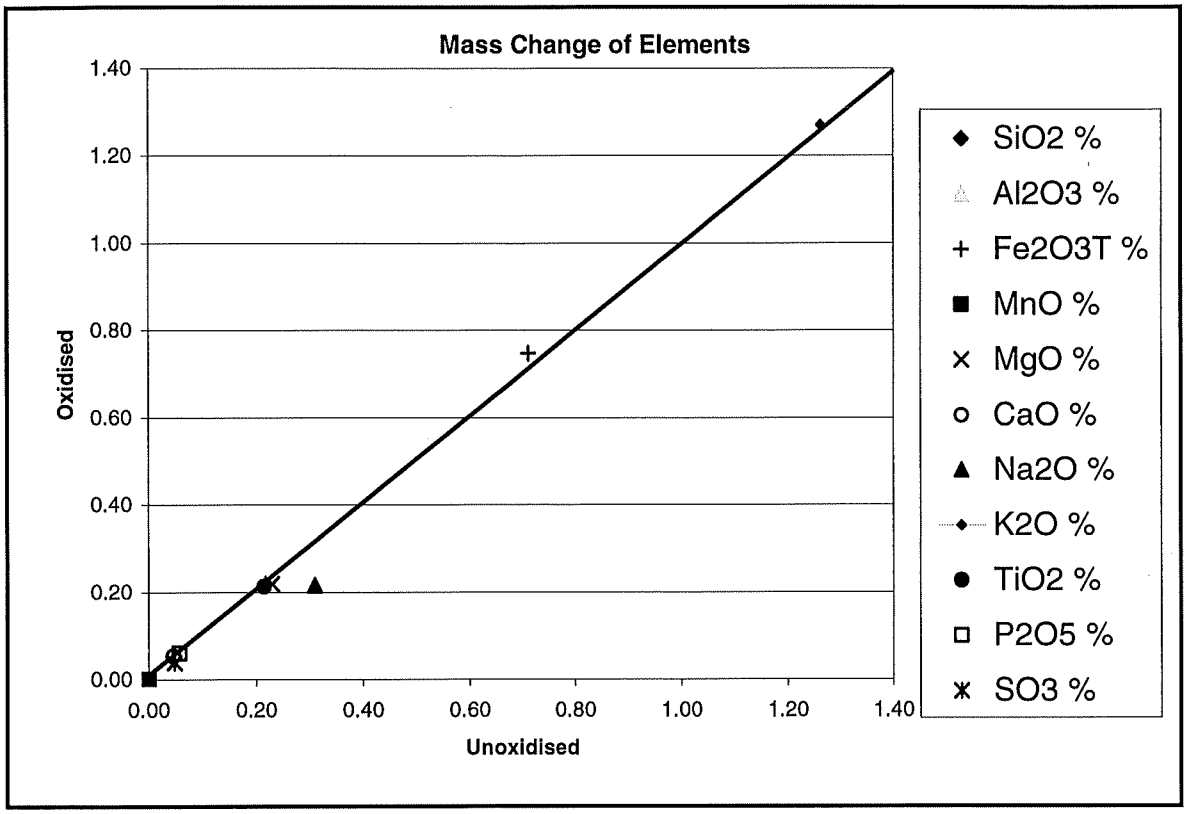

Figure 22. Diagram to illustrate the mass change between the oxidation and reduced zone. Elements that fall below the inert zircon line have under gone some degree of weather.

The elements that plot below the Zr line from the origin to the Zr point have to some extent become depleted during weathering or chemical alteration / oxidation processes.

Mass change (%) = $((C_i^O / C_i^{UN})*(C_{ZR}^{UN} / C_{ZR}^O) - 1] * 100$ **(1)**

Where C_i^O is the concentration of elements i in the oxidised zone, C_i^{UN} the concentration of element i in the unoxidised zone, C_{ZR}^{UN} is the concentration of Zr in the unoxidised zone. C_{ZR}^O is the concentration of Zr in the oxidised zone (Holmström et al., 2000).

The mass change in the major elements in the sandy yellow horizons (oxidised zone) is 4.93 % compared to the major elements in the dark green/grey horizons (reduced zone).

This suggests that weathering has played very little part in the distribution of elements between the sandy yellow horizons (oxidised zone) with the composition of the dark green/grey horizons (reduced zone). Due to weathering having minimal impact on the distribution of elements within the upper 0 – 2 m a possible explanation for the increased concentration at Mount Gunson as seen in Figure 13 – 16 is a function of climate, due to reduced rainfall and increased evaporation rates (Figure 12).

Oxidation zone

Studies by Jambour (1994) & Bernhard and Fontboté (2001) have shown that in evaporative dominated systems the water-soluble secondary salts chalcanthite, melanterite, anglesite and goslarite are the dominant secondary minerals to be found in the oxidation zone. The driving force for element concentration in the oxidation zone 0 – 2 m is capillary migration and evaporation Ritcey (1989) &. Bernhard and Fontboté (2001). With increasing evaporation the water flow direction changes to an upward migration via capillary forces (Figure 23).

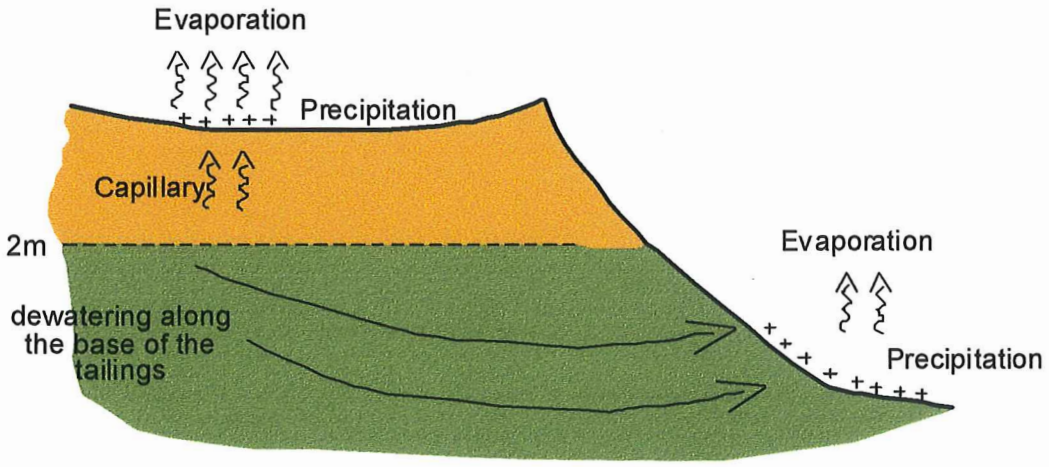

Figure 23 Showing the pathway for dewatering and evaporation in the Mount Gunson tailings and the migration of the water-soluble salts to the surface.

The migration of meteoric water interacts with the available oxygen and sulphides, as follows:

$FeS_2 + 7/2O_2 + H_2O \rightarrow Fe_2+ + 2SO_4^{2-} + 2H^+$ (oxygen path)

$FeS_2 + 14Fe^{3+} + 8H_2O \rightarrow 15Fe^{2+} + 2SO_4^{2-} + 16H^+$ (ferric iron path)

$CuFeS_2 + 4O_2 \rightarrow Fe^{2+} + Cu^{2+} + SO_4^{2-}$ (oxygen path)

$CuFeS_2 + 16Fe^{3+}\ 8H_2O \rightarrow 17Fe^{2+} + Cu^{2+} + 2SO_4^{2-} + 16H^+$ (ferric iron path)

These interactions lead to the liberation of bivalent cations for example Cu^{2+}, Zn^{2+}, Fe^{2+} and oxyanions such as SO_4^{2-}, and these cation and anion rich waters migrate to the surface through capillary action. Evaporation results in increased concentrations in the upper oxidation zone and finally precipitation of chlorides and sulphates (Figure 24 a). Dewatering from the base of the tailing embankments also results in the precipitation of chlorides and sulphates through evaporation (Figure 24 b).

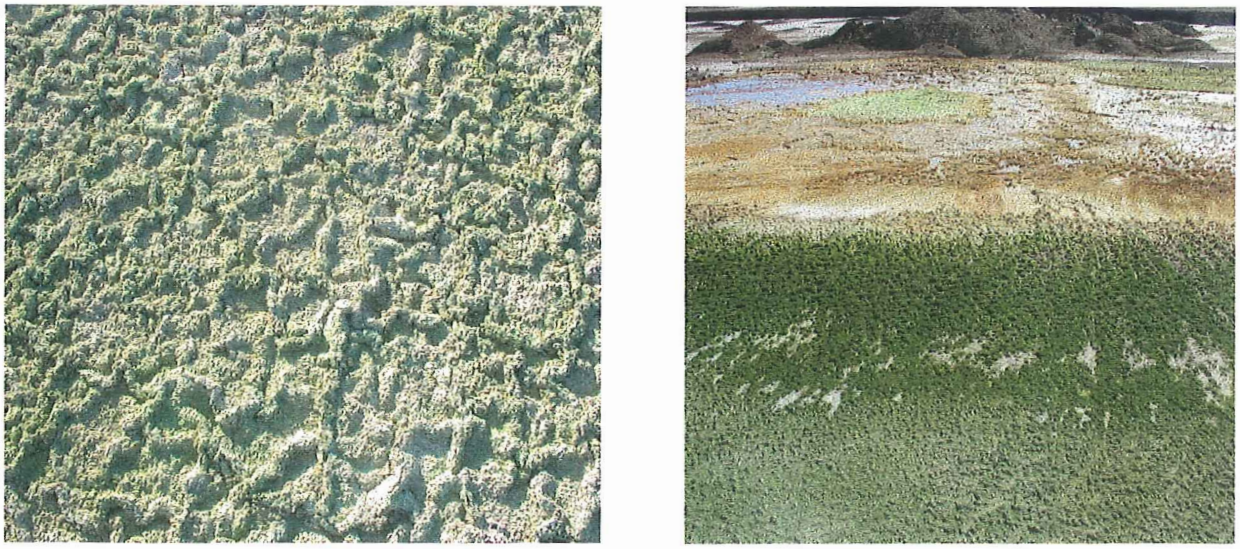

(a) (b)

Figure 24 precipitations of soluble salts on the upper surface of the tailings (a), and from the dewatering at the base of the tailing embankment (b)

Reduced zone

A possible explanation for the variation in element concentrations within the reduced environment (2 – 8 m) of impoundment 1 (Figure 13) is expected to be a function of:

1. Mineral and grain size partitioning upon deposition in the tailings.

Reduced zone

A possible explanation for the variation in element concentrations within the reduced environment (2 – 8 m) of impoundment 1 (Figure 13) is expected to be a function of:

1. Mineral and grain size partitioning upon deposition in the tailings.
2. The grade of ore being mined
3. Efficiency of the extraction process.

Grain size variation for MGL, MGF, MGA and MGB was minimal with a relatively constant grain size of 0.33 mm with depth, due to a thickened tailings being discharged, resulting in a relatively homogenous deposit. This suggests that mineral partitioning during deposition is not the cause for the variation in element concentration.

Tonkin & Creelman (1990) (Figure 4) have shown that the Cattle Grid deposit consisted of a chalcocite rich ore flanked on the west by a lower grade ore containing bornite and chalcopyrite. From this we might speculate that during initial stages of mining and extraction 1972 - 1974 mainly the rich chalcocite ore was processed, with ore being extracted from a transitional zone between the rich chalcocite and less economical bornite and chalcopyrite containing ore in the latter stages of mining in 1976. Therefore the copper fluctuations observed at depth in geochemical profile MGL are reflecting the mining compositionally varying ore in this transitional zone. Further, extraction processes at the time may have been favouring the recovery of the chalcocite over the bornite and chalcopyrite, resulting in a relative concentration of bornite and chalcopyrite into the tailings along with pyrite, sphalerite, galena and carrollite. Information gathered suggests that at the time the flotation cell capacity was inadequate and that the residence time of 9 minutes resulted in poor recovery rates of 86.2 % (Bradshaw 1984, D. O' Callaghan, pers.comm).

A possible explanation for the negligible fluctuation and decrease in copper concentration to depth for impoundments 2 & 3 as seen in (Figure 14 – 16) maybe that at the time of mining the ore consisted of the less economical minerals bornite and chalcopyrite. As a reaction to the fluctuating copper prises during 1976 – 1986 (Figure 25), additional cells for the flotation process were implemented, to ensure maximum copper recovery (Bradshaw, 1984). This resulted in average recoveries of 92.71 %, and these high recovery rates resulted in reduced copper concentrations in the tailings.

Regolith map

It was hoped that from the regolith map a relationship between copper concentration and landforms, might arise. It turned out there was no relationship and this is possibly due to the minimal relief over the surface of the tailings.

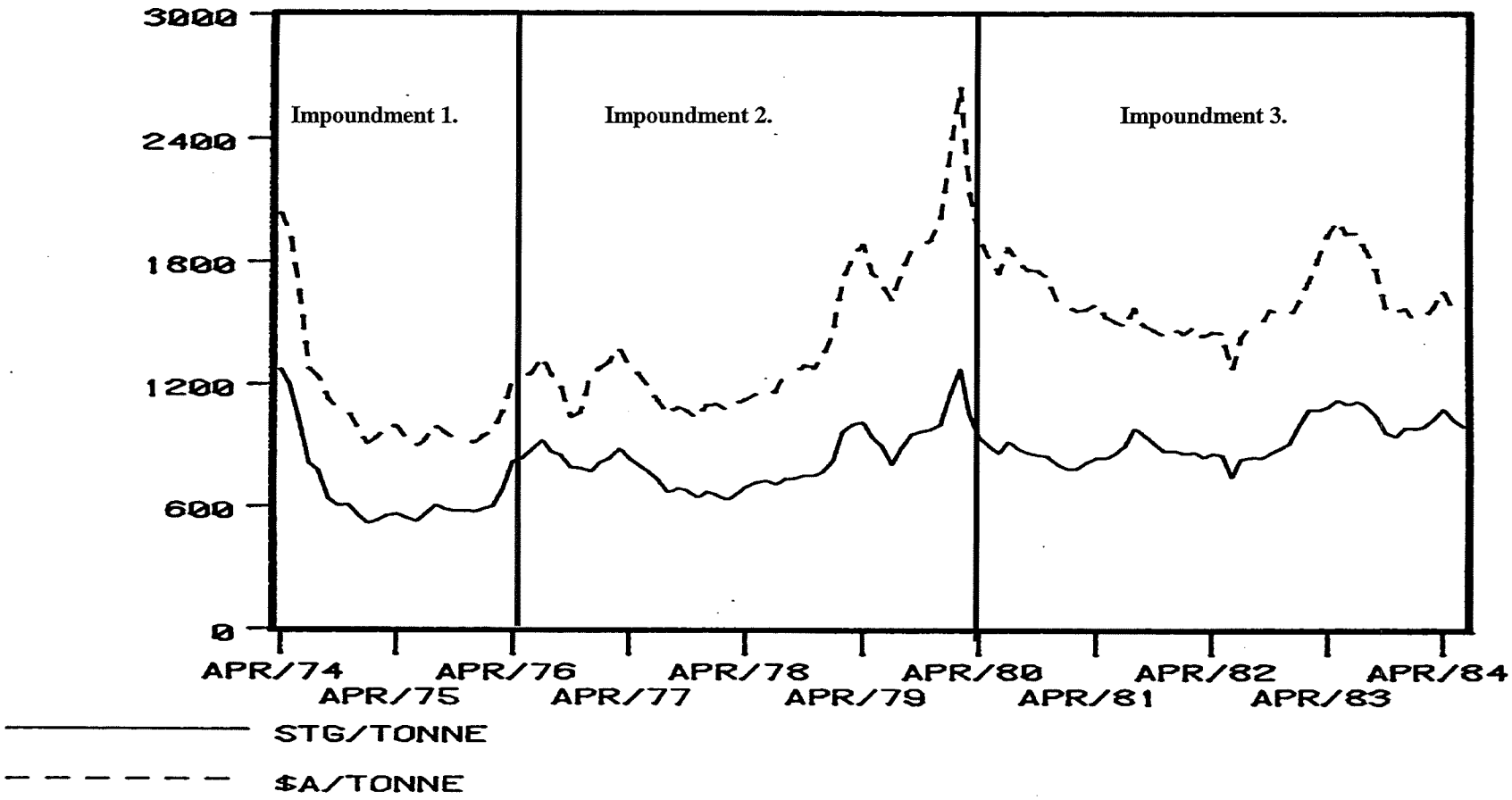

Figure 25: Copper prices for the period of 1974 – 1985.

Conclusion

Vertical sections of the Mount Gunson tailing deposit revealed two distinct zones. The upper region from 0 – 2 m is dominated by sandy golden horizons with an average pH of 5. Metals released from the oxidation of sulphide minerals are transported to the upper surface through evaporation via capillary action, resulting in elevated concentrations of copper in the form of chlorides and sulphates. The lower region 2 m to bottom of the core is dominated by green/grey horizons with an average pH of 7 – 8. It appears that sulphides in the reduced environment are less conducive to corrosion. Present day variation of copper concentrations within the reduced environment of the tailings are suggested to be a reflection of the ore grade being extracted, and efficiencies within the extraction process.

Acknowledgements

I would like to thank Daniel Radulovic and Sean Mahoney for helping in the field. The Musolino company for allowing us to stay on site. Andreas Schmidt-Mumm for his input into my draft. A special thanks to my family for their support throughout the year.

TABLE OF FIGURES

Figure 8. Aerial photo showing location of cores obtained, MGL (1), MGF (2), MGA and MGB (3).

Figure 9. RKS drilling equipment used to extract core from the three impoundments MGL, MGF, MGA and MGB.

Figure 10. pH vrs depth (m) within the three tailings MGL (a), MGF (b), MGA (c) and MGB (d). Reveals that as depth increases pH increases.

Figure 11. Illustrating moisture content throughout the tailings. (a) MGF, (b) MGA and (c) MGB.

Figure 12. Precipitation and evaporation rates at the Woomera airfield 2002.

Figure 13. Geochemical profile for element distribution through impoundment 1 MGL. Concentrations at depths represent the bulk sample for that 1 m core (eg: Cu 1113 ppm is concentration for the depth O – 1 m). Note: Ni has been multiplied by 10 for observation purposes.

Figure 14. Geochemical profile for element distribution through impoundment 2 inner rim MGF. Concentrations at depths represent the bulk sample for that 1 m core (eg: Cu 2139 ppm is concentration for the depth O – 1 m). Note: Ni has been multiplied by 10 for observation purposes.

Figure15. Geochemical profile for element distribution through impoundment 3 outer rim MGA. Concentrations at depths represent the bulk sample for that 1 m core (eg: Cu 1110 ppm is concentration for the depth O – 1 m). Note: Ni has been multiplied by 10 for observation purposes.

Figure 16. Geochemical profile for element distribution through impoundment 3 inner rim MGB. Concentrations at depths represent the bulk sample for that 1 m core (eg: Cu 2564 ppm is concentration for the depth O – 1 m). Note: Ni has been multiplied by 10 for observation purposes.

Figure 17. Pyrite grain displaying highly fractured corroded surfaces in the upper 2 m.

Figure 18. Variable degrees of corrosion between bornite and chalcopyrite in the upper 2 m. (a) bornite, (b) chalcopyrite.

Figure 19. Primary sulphides at depths below 2 m revealing well defined edges free from corrosion. (a) chalcopyrite, (b) bornite, (c) covellite and (d) sphalerite.

Figure 20. Bornite displaying alternating layers with chalcopyrite and small patches of covellite at a micrometer scale. (1) covellite, (2) bornite and (3) chalcopyrite.

Figure 21. Copper boundaries and the relationship of compositional variation of the ore minerals in the tailings. (a) iron (b) zinc and (c) cobalt & nickel.

Figure 22. Diagram to illustrate the mass change between the oxidation and reduced zone. Elements that fall below the inert zircon line have under gone some degree of weather.

Figure 23. Showing the pathway for dewatering and evaporation in the Mount Gunson tailings and the migration of the water-soluble salts to the surface.

Figure 24. (a) Precipitation of the soluble salts on the upper surface of the tailings, and (b) from the dewatering at the base of the tailing embankment.

Figure 25. Copper prices for the period of 1974 – 1985.

References

Bampton K.F., 1988. Adelaide Chemical Co., Mt Gunson, Miner. Ind. Q. South Aust., 51:21.

Bernhard, D., and Fontboté, L., 2001. Element cycling and secondary mineralogy in porphyry copper tailings as a function of climate, primary mineralogy, and mineral processing. Journal of Geochemical Exploration. 74, pp 3 – 55.

Boulet, M.P., Adrienne, C., Larocque, L., 1998. A comparative mineralogical and geochemical study of sulfide mine tailings at two site in New Mexico, USA. Evnironmental Geology 33, 130 – 142.

Bradshaw, P.C., 1984 Mount Gunson Mines, A review of the Mount Gunson Concentrator. In: CSR Mount Gunson Mines operations review for 1974 – 1984.

Busbridge, M., 1981. An analysis of the sedimentary host rocks and mineralization at the Cattle Grid orebody, Mt Gunson, B.Sc (Hons) thesis (unpublished), The University of Adelaide.

Callaghan D. O', 2002 personal communication, Mine site manager, Mount Gunson.

Deer, W.A., Howie, R.A and Zussman, J. 1992. An Introduction to the Rock – Forming Minerals second edition. Co- published John Wiley & Sins Inc., 605 Thrid Avenue, New York, NY 10158.

Dickson, S.B., 1942. Copper deposits of South Australia, Geol. Surv. South Aust. In: Geological Aspects of the Discovery of Some Important Mineral Deposits in Australia. Monograph Series 17. pp. 113 – 119.

Gersteling, R.W and Heape, J.M., 1975. The Cattle Grid orebody, Mount Gunson, South Australia, in South Australian Conference, 1975, pp. 103 – 112 (The Australasian Institute of Mining and Metallurgy: Melbourne)

Holmström, H., Ljungberg, J., Ekström, K., Öhlander, B., 1999. Secondary copper enrichments in tailings at the Laver mine, north Sweden. Environ. Geol. 38, 1 – 16.

Houston, M.L., 1977. Mining operations at the Cattle Grid copper deposit – Mount Gunson, Miner Resources. Rev. South Aust., 141: 64 – 68.

Jambour, J.L., 1994. Mineralogy of sulfide-rich tailings and their oxidation products. In: Jambour, J.L., Blowes, D.W. (Eds.), Short Course Handbook on Environmental Geochemistry of Sulfide Mine Waste. Mineralogical Association of Canada. Nepean, vol. 22. pp. 59 – 102.

Knuts, J., Donelly, T.H and Tonkin, D.G., 1983. Geochemical constraints on the genesis of copper mineralization in the Mount Gunson area, South Australia, Econ. Geol., 78: 250 – 274.

Lambert, I.B., Donnelly, T.M. and Etminan, H., 1984. The Diverse Styles of Sediment-Hosted Copper Deposits. In: Geology and Metallogeny of Copper Deposits, Proceedings of the Copper Symposium 27th International Geological Congress Moscow, 1984. pp 540 – 558.

Lintern, M.J., Sheard, M.J., and Gray, D.J., 1998. Geochemical studies of the regolith at the Mt Gunson copper deposits, Stuart Shelf, South Australia. In: CRCLEME report 76R.

Madien, K.J., 1989. Structural traps for stratrabound copper deposits in the Mount Gunson area, South Australia. In: Boyle, R.W., Brown, A.C., Jefferson, C.W., Jowett, E.C. and Krikham, R.V., eds., Sediment hosted Stratiform Copper Deposits: Geological Association of Canada, Special Paper 36, p 543 – 554.

Pain C, Chan R, Craig M, Gibson D, Ursem P, Wilford J (2000) RTMAP Regolith Database filed and users guide, 2nd Edition, CRC LEME Report 138

Puccini, O., 1996. Assessment of Remedial Operations Mt Gunson Tailings Facility. pp 1 – 18.

Preiss, W.V., (Comp.), 1987. The Adelaide Geosyncline: Late Proterozic stratigraphy, sedimentation, palaeontology and tectonics, Geol.Surv. South Aust. Bull., 53: 384 – 389.

Rattigan, J.H., 1988. The Cattle Grid deposit. In: Geological Aspects of the Discovery of Some Important Mineral Deposits in Australia. Monograph Series 17. pp. 121 – 124.

Ritcey, G.M., 1989. Mobility – Migration and Salt Formation by capillary Action. In: Tailings management problems and solutions in the mining industry. Published Elsevier 1989. Pages 329 – 349.

Solomon, M., and Groves, D.I., 1994, The Geology and Origin of Australia's Mineral Deposits: Oxford University Press, 951 pp.

Tonkin, D.G. and Creelman, R.A., 1990. Mount Gunson copper deposits, in Geology of Mineral Deposits of Australia and Papua New Guinea (Ed. F.E. Hughes), pp 1037 – 1043 (The Australasian Institute of Mining and Metallurgy: Melbourne)

Van Herk, H., Houston, M.L and Dudgeon, R.N., 1975. Planning development and extraction of the Cattle Grid ore deposit, Mt Gunson, in South Australia Conference, 1975, pp. 113 – 124 (The Australasian Institute of Mining and Metallurgy: Melbourne)

Woodburn Fitzhardinge Geotechnical Consulting Engineers, 1987.Mount Gunson tailings dams.

www.bom.gov.com

Appendix 1

Site: Tailings impoundment 1 (MGL)

Location MGL 706736 (E) 6520418 (N) outer edge of impoundment 1

Accuracy: 5m

Sample ID	Average depth (m)	Description
MGL	0-0.1	Dry 10 YR 7/4 The core is dominated by sandy golden hue, with the grain size medium / coarse.
MGL	0.1 – 0.2	Dry 7.5 YR 7/4 Sample is very burnt orange / red with a relatively coarse fraction which then blends into a creamy / white region (leached)
MGL	0.2 – 0.4	Dry 10 YR 7/4 The core is dominated by sandy golden hue, with the grain size medium / coarse.
MGL	0.4 – 0.6	Dry 10 YR 7/4 The core is dominated by sandy golden hue, with the grain size medium / coarse.
MGL	0.6 – 0.90	Dry 10 YR 7/4 The core is dominated by sandy golden hue, with the grain size medium / coarse.
MGL	0.90 – 1.25	Dry 10 YR 7/4 The core is dominated by sandy golden hue, with the grain size medium / coarse.
MGL	1.25 – 1.50	Dry 10 YR 7/4 The core is dominated by sandy golden hue, with the grain size medium / coarse.
MGL	1.50 – 1.75	Dry 7.5YR 7/2 Very coarse grained; The majority of the core is of a grey colour.
MGL	1.75 – 2.19	Dry 2.5 YR 7/3 Medium fraction, we have a distinct layer of purple / grey.
MGL	2.19 – 2.75	Dry 2.5 YR 7/3 Medium fraction, we have a distinct layer of purple / grey.
MGL	2.75 – 3.25	Dry 10 YR 7/2 Thick distinct grey fraction of medium / coarse sediments.
MGL	3.25 – 3.75	Dry 7.5 YR 7/2 Medium / coarse, homogeneous grey / purple layers.
MGL	3.75 – 4.25	Dry 7.5 YR 7/2 Medium / coarse, homogeneous grey / purple layers.
MGL	4.25 – 4.75	Dry 2.5 YR 7/3 Medium fraction, we have a distinct layer of purple / grey.
MGL	4.75 – 5.25	Dry 7.5 YR 7/3 The fraction is medium / coarse, homogeneous grey / purple layers.
MGL	5.25 – 5.75	Dry 7.5 YR 7/3 The fraction is medium / coarse, homogeneous grey / purple layers.
MGL	5.75 – 6.75	Dry 7.5 YR 7/3 The fraction is medium / coarse, homogeneous grey / purple layers.
MGL	6.75 – 7.75	Dry 7.5 YR 7/3 The fraction is medium / coarse, homogeneous grey / purple layers.
MGL	7.75 – 8.75	Dry 7.5 YR 7/3 The fraction is medium / coarse, homogeneous grey / purple layers.

Site: Tailings impoundment 2 (MGF)
Location: 0707079 (E) 6520229 (N)
Accuracy: 6m

Sample ID	Average depth (m)	Description
MGF	0-1	Dry 10 YR 7/4 The core is dominated by sandy golden hue, with the grain size medium / coarse.
MGF	1-2	Dry 7.5 YR 7/4 Sample is very burnt orange / red with a relatively coarse fraction which then blends into a creamy / white region (leached)
MGF	2-3	Dry 2.5 YR 7/3 Medium fraction, we have a distinct layer of purple / grey.
MGF	3-4	Dry 10 YR 7/2 Thick distinct grey fraction of medium / coarse sediments.
MGF	4-5	Dry 7.5 YR 7/2 Medium / coarse, homogeneous grey / purple layers.
MGF	5-6	Dry 7.5 YR 7/3 The fraction is medium / coarse, homogeneous grey / purple layers.
MGF	6-7	Dry 7.5YR 7/2 Very coarse grained; The majority of the core is of a grey colour.

Site: Tailings impoundment 3 (MGA)
Location: 0707332 (E) 6520411 (N)
Accuracy: 5m

Sample ID	Average depth (m)	Description
MGA	0-1	Dry 10 YR 7/4 The core is dominated by sandy golden hue, with the grain size medium / coarse.
MGA	1-2	Dry 7.5 YR 7/4 Sample is very burnt orange / red with a relatively coarse fraction which then blends into a creamy / white region (leached)
MGA	2-3	Dry 2.5 YR 7/3 Medium fraction, we have a distinct layer of purple / grey.
MGA	3-4	Dry 10 YR 7/2 Thick distinct grey fraction of medium / coarse sediments.
MGA	4-5	Dry 7.5 YR 7/2 Medium / coarse, homogeneous grey / purple layers.
MGA	5-6	Dry 7.5 YR 7/3 The fraction is medium / coarse, homogeneous grey / purple layers.
MGA	6-7	Dry 7.5YR 7/2 Very coarse grained, The majority of the core is of a grey colour.
MGA	7-8	Dry 7.5 YR 7/2 The core is homogeneous in texture throughout the 1 m section with a grain fraction of fine → medium.
MGA	8-9	Dry 7.5 YR 8/1 The grain fraction medium grained. With the colour being a distinct grey with fine mottling of purple.
MGA	9-10	Dry 10 YR 7/2 Very coarse grained, The majority of the core is of a grey colour

Site: Tailings impoundment 3 (MGB)
Location: 0707187 (E) 6520477 (N)
Accuracy: 5m

Sample ID	Average depth (m)	Description
MGB	0-1	Dry 10YR 7/2 Grain size is considered to be medium grained. Throughout the core we can see quite clear speckles of green grains.
MGB	1-2	Dry 7.5 YR 7/3 The core is homogeneous in texture throughout the 1 m section with a grain fraction of fine → medium.
MGB	2-3	Dry 7.5 YR 7/3 The core is homogeneous in texture throughout the 1 m section with a grain fraction of medium.
MGB	3-4	Dry 5 YR 7/3 Core is very medium→ fine fractions with interdispersed purple grains.
MGB	4-5	Dry 7.5 YR 7/3 The grain fraction medium grained. With the colour being a distinct grey with fine mottling of purple.
MGB	5-6	Dry 7.5 YR 8/2 The grain fraction coarse with a distinct grey colour with fine mottling of purple.
MGB	6-7	Dry 5 YR 8/2 The core is homogeneous in texture throughout the 1 m section with a grain fraction of medium.

Appendix 2.

XRF major element data.

16/05/2002 10:48 MAJOR ELEMENT ANALYSES Page: 1- 1

Sample Name	SiO2 %	Al2O3 %	Fe2O3T %	MnO %	MgO %	CaO %	Na2O %	K2O %	TiO2 %	P2O5 %	SO3 %	LOI %	Total %
2032-MGL01	89.33	4.73	0.61	0.00	0.21	0.03	0.39	0.95	0.20	0.05	0.06	1.83	98.41
2032-MGL02	93.64	3.37	0.52	0.00	0.12	0.02	0.15	0.66	0.16	0.04	0.00	1.18	99.86
2032-MGL03	89.12	4.12	0.58	0.00	0.17	0.04	0.33	0.81	0.18	0.05	0.04	1.71	97.15
2032-MGL04	88.15	6.62	0.62	0.00	0.26	0.10	0.33	1.43	0.22	0.06	0.06	2.16	100.01
2032-MGL05	87.93	5.57	0.56	0.00	0.20	0.03	0.22	1.20	0.20	0.05	0.02	1.78	97.77
2032-MGL06	85.32	7.26	0.88	0.00	0.27	0.04	0.31	1.54	0.25	0.06	0.05	2.57	98.55
2032-MGL07	84.30	8.27	0.73	0.00	0.33	0.05	0.46	1.85	0.25	0.07	0.09	2.79	99.19
2032-MGL08	86.71	7.20	0.85	0.00	0.23	0.04	0.29	1.31	0.23	0.06	0.03	2.77	99.72
2032-MGL09	84.01	7.81	1.02	0.00	0.29	0.05	0.40	1.61	0.25	0.07	0.09	2.97	98.57
2032-MGL010	89.23	5.38	0.80	0.00	0.20	0.03	0.21	1.13	0.20	0.05	0.03	1.91	99.18
2032-MGL011	88.61	5.35	0.77	0.00	0.21	0.05	0.44	1.08	0.20	0.05	0.08	1.98	98.82
2032-MGL012	87.83	5.40	0.75	0.00	0.20	0.06	0.25	1.06	0.20	0.05	0.09	1.86	97.77
2032-MGL013	88.43	5.69	0.69	0.00	0.20	0.05	0.25	1.05	0.20	0.06	0.03	2.07	98.70
2032-MGL014	81.76	9.84	0.91	0.00	0.35	0.09	0.36	1.98	0.27	0.08	0.03	3.10	98.79
2032-MGL015	87.26	6.69	0.68	0.00	0.22	0.06	0.19	1.33	0.21	0.07	0.03	2.15	98.90
2032-MGL016	85.11	7.15	0.77	0.00	0.23	0.07	0.17	1.45	0.23	0.07	0.05	2.13	97.43
2032-MGL017	88.06	6.11	0.69	0.00	0.20	0.04	0.12	1.20	0.21	0.06	0.02	1.87	98.59
2032-MGL018	88.10	6.14	0.72	0.00	0.20	0.04	0.08	1.24	0.21	0.06	0.01	1.84	98.63
2032-MGL019	88.65	5.72	0.70	0.00	0.18	0.04	0.08	1.17	0.20	0.06	0.01	1.72	98.52
2032-DAN01	89.85	4.20	0.68	0.00	0.15	0.05	2.45	0.88	0.19	0.05	0.03	1.72	100.26
2032-DAN02	85.65	3.46	1.09	0.01	0.50	2.89	0.17	0.48	0.24	0.05	0.61	3.62	98.76
2032-DAN03	85.38	3.27	0.99	0.01	0.54	3.48	0.14	0.36	0.26	0.05	0.47	4.08	99.02

16/05/2002 10:48 MAJOR ELEMENT ANALYSES Page: 1- 2

XRF trace element data.

Trace Element Analyses for Karen Hulme, May 2002

SAMPLE	Zr ppm	Y ppm	Sr ppm	Rb ppm	U ppm	Th ppm	Pb ppm	Ga ppm	Cu ppm	Zn ppm	Ni ppm	Ba ppm	Sc ppm	Co ppm	V ppm	Cr ppm	
2032-MGL01	182.4	12.7	205.8	29.3	1.7	14.2	47.2	5.8	848	213	22	117	2.0	493	22	17	
2032-MGL02	172.4	11.0	174.6	20.3	1.5	11.8	42.1	4.9	447	136	11	109	1.9	239	18	13	
2032-MGL03	170.0	12.0	199.1	24.9	1.3	12.7	74.8	5.7	726	200	15	107	1.5	236	19	16	
2032-MGL04	172.7	13.3	244.4	43.9	1.6	15.5	80.0	8.1	966	154	18	137	1.9	306	21	21	
2032-MGL05	169.6	13.0	224.0	37.5	1.5	13.8	116.7	7.7	967	184	23	142	2.0	263	19	23	
2032-MGL06	202.6	15.2	262.4	46.8	2.5	21.9	388.6	8.5	2727	412	32	146	2.1	349	26	61	
2032-MGL07	195.7	16.0	291.8	57.0	1.9	18.0	90.6	11.1	1666	306	23	171	1.4	242	22	47	
2032-MGL08	188.7	13.9	269.8	40.2	2.5	23.9	415.6	9.5	2574	471	31	149	2.3	381	24	31	
2032-MGL09	198.5	15.3	271.9	49.2	1.8	23.5	309.7	8.6	2951	674	36	200	2.1	486	26	31	
2032-MGL10	181.9	12.7	206.5	35.7	1.8	17.2	216.0	7.6	1348	725	23	173	2.3	273	18	28	
2032-MGL011	181.4	12.0	212.9	34.0	1.4	19.3	279.1	8.3	1502	830	18	149	1.8	199	20	30	
2032-MGL012	174.9	12.1	215.7	33.0	2.4	18.3	260.9	7.4	2039	673	14	172	1.9	144	18	24	
2032-MGL013	167.9	11.8	235.6	33.0	1.3	18.6	225.5	6.8	1169	502	17	167	1.1	204	20	24	
2032-MGL014	184.9	15.8	363.2	60.2	1.8	26.8	373.2	11.5	1590	681	18	323	2.6	182	26	35	
2032-MGL015	168.1	13.1	284.4	40.6	2.4	21.3	237.7	8.1	1527	532	15	248	2.2	132	20	26	
2032-MGL016	172.5	14.4	279.5	45.7	2.0	30.3	399.8	9.8	3075	979	12	220	2.6	64	33	30	
2032-MGL017	169.6	12.2	245.2	37.9	1.7	24.3	260.8	8.3	1939	625	11	181	2.6	90	30	29	
2032-MGL018	159.5	10.8	247.0	39.1	1.8	16.7	167.5	8.3	993	412	19	232	1.7	189	20	39	
2032-MGL019	173.1	12.0	240.2	37.0	1.5	20.2	236.2	7.5	1822	542	12	197	2.0	108	24	31	

Appendix 3

Mt Gunson Anthropogenic Regolith –Landform Map Units.

Afa1*: Sub-angular medium grained homogeneous quartzose sand. Surface is a very light green ~ 0-5 mm in thickness, upon removal the lower grains show a hue of orange/brown sub-angular sand. No visible vegetation.

Afa2*: Sub-rounded medium grained quartzose sand. Surface is a very light green ~ 0-4 mm in thickness. No visible vegetation. (Possibly relating to old tailing material washing into Gunyah Lake).

Afa3*: Sub angular-rounded sand ~ 300 microns. Surface is transparent to pink (Pandurra), with light green tinge throughout with cementation between grains. No visible vegetation. (Possibly relating to old tailing material washing into Gunyah Lake).

Apd1*: Sub-angular medium grained quartzose sand. Fe-oxide coating on the some quartzose grains. The upper-surface has a distinct green while lower regions are still orange/brown. Salt crusts on some surfaces. No visible vegetation.

Aaw1*: Dominate fine-grained brown clay with minor sub-angular quartzose grains. No visible vegetation.

Aaw2*: Fine grained clay-silt, pale green white coloured sediment, with fien grained sand. No visible vegetation on the tailings.

Aaw3: Fine grained brown clay, with minor sub-angular quartzose grains. No visible vegetation. (Natural Salt Lake Surface).

Aca: Sub-angular-rounded medium grained quartzose sand, red brown sands. Colonised by Chenopod shrubs dominated by *Atriplex vesicaria, Atriplex stipitata, Atriplex spongiosa*, with minor *Eremophila* tree ssp.

Aer1*: Sub-angular medium grained quartzose sand, surface green/purple/yellow, at depth orange/brown. No visible vegetation.

Cer1*: Sub-angular to rounded course grained quartzose sand, white/green sand, with minor, quartzite and secrete material. No visible vegetation.

Cer2*: Sub-angular course grained quartzose sand, white-brown. Dominant quartzite material rock material. No visible vegetation (historic stockpiles in East and West Lagoon).

CHer: Sub rounded fine grained quatzose sand, red brown sand, with rounded gravel and stones mainly quartzite and silcretes. Colonised by Chenopod shrubs dominated by *Atriplex vesicaria, Atriplex stipitata, Atriplex spongiosa*, with minor *Maireana* and *Scleroleana spp.*

Isu1: Sub-rounded medium grained quatzose sands, red brown sands, with occasional courser sands. Colonised by *Acacia aneura, Dodonaea viscosa ssp. angustissima, Acacia ligulata, Enchylaena tomentosa* with various *Atriplex spp.*

Ips1: Sub-rounded medium grained quatzose sands, red brown sands, with occasional courser sands, within low relief areas. Colonised by *Acacia aneura, Acacia papyrocarpa, Acacia ligulata, Dodonaea viscosa ssp. angustissima*, various *Atriplex* spp with the native pine *Callitris columellaris.*

SSer: Outcropping quartzose rich Pandurra Formation. Colonised by succulants.

Water bodies*: Copper enriched water.

Tailing Bund*: Sub-rounded medium grained quatzose sand, red brown sand. Making the perimeter of the surface of the tailing.

Old Tailing/Stock Pile*: Black fine grained course grained, gravel like capping of stockpile/tailings. 15m high.

Disturbed*: Surrounding stockpile, tailings and East and West Lagoon. Medium green on Mt Gunson Anthropogenic Regolith–Landform Map.

* = Anthropogenic material, deposited or influenced directly or indirectly by human induced activity.

Regolith
Transported Regolith
A = Alluvial Sediment (Natural and Anthropogenic)
C = Colluvial Sediment (Natural and Anthropogenic)
I = Aeolian Sediment (Natural)
In-Situ Regolith
SS = Slightly weathered bedrock
Landforms

fa =	alluvial fan	ca =	channel deposit	ps = sandplain
pd =	depositional plain	er =	erosional rise	
aw =	alluvial swamp	su = dune field		

Mount Gunson Anthropogenic Regolith-Landform Map

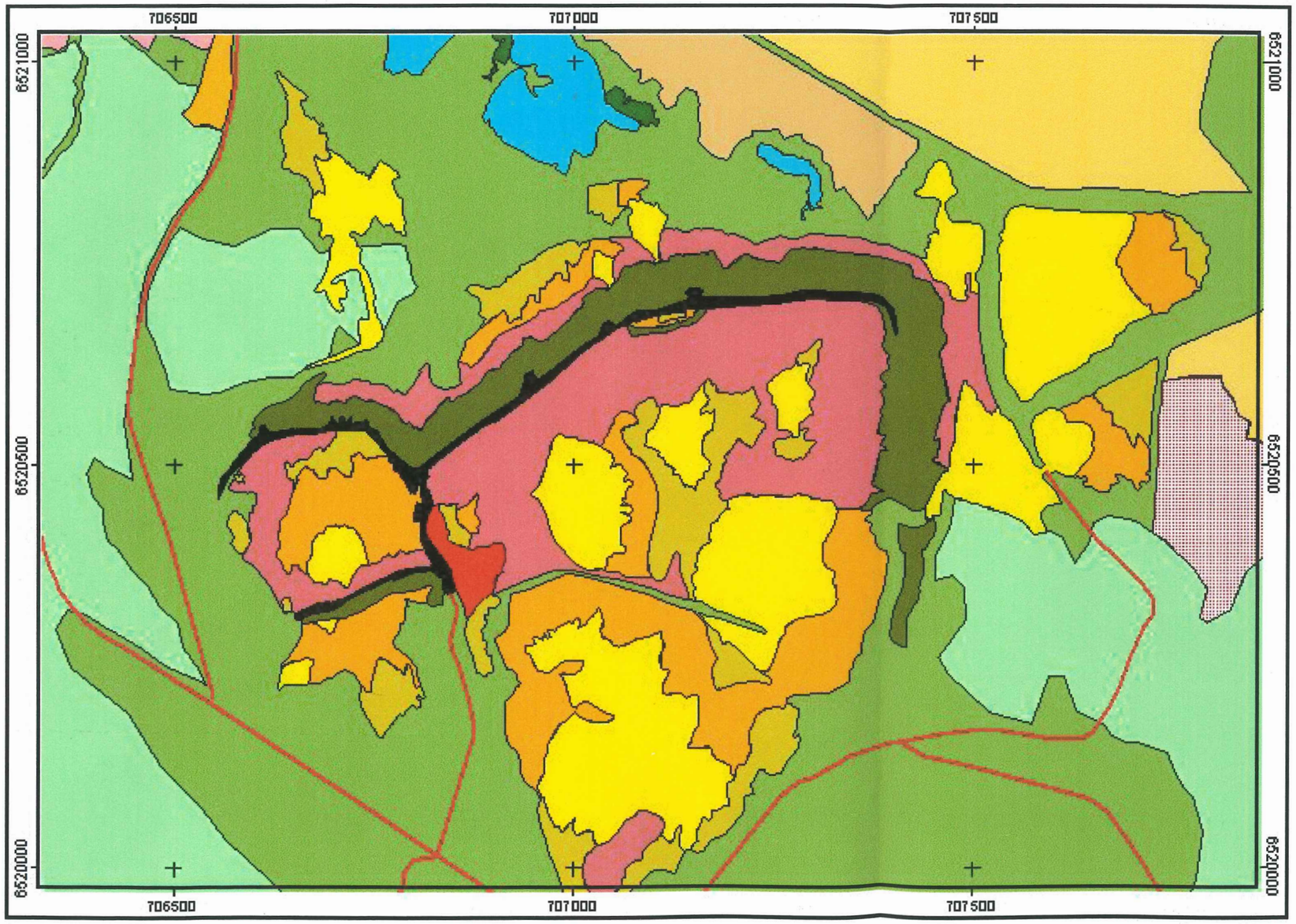

Legend

- Road
- Afa 1
- Afa 2
- Afa 3
- Apd 1
- Apd 2
- Aaw 1
- Aaw 2
- Aaw 3
- Aca.shp
- Maer 1
- Maer 2
- Cer 1
- Cer 2
- Isu
- Pld
- CHer
- Cmm
- Tailings wall
- Waterbodies
- SSer

N

0 500 1000 1500 2000 Meters